FRACTURE CHARACTERIZATION AND FRACTURE-PERMEABILITY ESTIMATION AT

THE UNDERGROUND RESEARCH LABORATORY IN SOUTHEASTERN MANITOBA, CANADA

By F. L. Paillet

U.S. GEOLOGICAL SURVEY

Water-Resources Investigations Report 88-4009

Denver, Colorado
1988

CONVERSION FACTORS AND ABBREVIATIONS

For use of readers who prefer to use inch-pound units rather than the metric (International System) units used in this report, the following conversion factors may be used:

Multiply metric unit	By	To obtain inch-pound unit
meter (m)	3.281	foot (ft)
centimeter (cm)	0.3937	inch (in.)
microsecond per meter (μs/m)	3.281	microsecond per foot (μs/ft)
square centimeter per second (cm^2/s)	0.00107639	square foot per second (ft^2/sec)
millimeter (mm)	0.03937	inch (in.)
kilometer (km)	0.6214	mile (mi)
square kilometer (km^2)	0.3861	square mile (mi^2)
kilometer per second (km/s)	0.6214	miles per second (m/s)
Liter (L)	0.2642	gallon (gal)
Liter per minute (L/min)	0.2642	gallon per minute (gal/min)

Temperature

degree Celsius (°C)	$°F = 1.8 \times °C + 32$	degree Fahrenheit (°F)

The following units are listed to define abbreviations:

kilohertz (kHz)

microsecond (μs)

second (s)

CONTENTS

FIGURES

TABLES

FRACTURE CHARACTERIZATION AND FRACTURE-PERMEABILITY ESTIMATION AT THE

UNDERGROUND RESEARCH LABORATORY IN SOUTHEASTERN MANITOBA, CANADA

Frederick L. Paillet
U.S. Geological Survey
Denver, Colorado 80225

ABSTRACT

Various conventional geophysical well logs were obtained in conjunction with acoustic tube-wave amplitude and experimental heat-pulse flowmeter measurements in two deep boreholes in granitic rocks on the Canadian shield in southeastern Manitoba. The objective of this study is the development of measurement techniques and data-processing methods for characterization of rock volumes that might be suitable for hosting a nuclear-waste repository. One borehole, WRA1, intersected several major fracture zones, and was suitable for testing quantitative permeability estimation methods. The other borehole, URL13, appeared to intersect almost no permeable fractures; it was suitable for testing methods for the characterization of rocks of very small permeability and uniform thermo-mechanical properties in a potential repository horizon. Epithermal neutron, acoustic transit time, and single-point resistance logs provided useful, qualitative indications of fractures in the extensively fractured borehole, WRA1. Most of these fractures corresponded to open fractures identified on core, and were confirmed by acoustic televiewer logs. The analysis indicates that a neutron log can provide indications of the extent of weathering, possibly related to the extent of ground-water movement. A single-point log indicates both weathering and the degree of opening of a fracture-borehole intersection. All logs indicate the large intervals of mechanically and geochemically uniform, unfractured granite below depths of 300 meters in the relatively unfractured borehole, URL13. Some indications of minor fracturing were identified in that borehole, with one possible fracture at a depth of about 914 meters in depth producing a major acoustic-waveform anomaly. Comparison of acoustic tube-wave attenuation with models of tube-wave attenuation in infinite fractures of given aperture provide permeability estimates ranging from equivalent single-fractured apertures of less than 0.01 millimeter to apertures of more than 0.5 millimeter. One possible fracture anomaly in borehole URL13 at a depth of about 914 meters corresponds with a thin mafic dike on the core where unusually large acoustic contrast may have produced the observed waveform anomaly. No indications of naturally occurring flow existed in borehole URL13; however, flowmeter measurements indicated flow at less than 0.05 liter per minute from the upper fracture zones in borehole WRA1 to deeper fractures at depths below 800 meters.

INTRODUCTION

The U.S. Geological Survey is conducting a long-term study of the application of borehole geophysics to the characterization of the hydrology of fractured crystalline rocks. Investigations of fractured rock hydrology have useful applications to such topics as regional recharge, ground-water circulation, contaminant migration, and earthquake mechanics. This study addresses those aspects of fracture mechanics and fracture hydrology relevant to the siting of a nuclear-waste repository. Host-rock masses considered suitable for high-level radioactive-waste storage would possess negligible permeability, so that possible waste migration would occur only by means of permeable fractures. Potential host rocks would be relatively strong when unfractured; however impermeable, sealed fractures would become potential locations for stress concentration and mechanical failure under thermo-mechanical stress fields induced by the stored waste.

Previous studies indicate that the mechanical and hydraulic properties of crystalline rocks are difficult to characterize using small core samples previously disturbed by drilling and subjected to release of tectonic and lithostatic stresses (Davison and others, 1982; Witherspoon and others, 1981). Borehole and surface-to-borehole geophysical techniques provide one of the primary means for identifying and characterizing fractures in situ. Therefore, continued development of such techniques will be a useful part of the technology needed to predict the performance of a nuclear waste repository established in crystalline rocks.

This report describes the analysis of geophysical log data obtained at a research site, the Underground Research Laboratory (URL), developed by Atomic Energy of Canada, Limited (AECL), for the testing of various techniques that might be used in characterizing crystalline rocks suitable for a nuclear-waste repository. Results of previous studies of geophysical logging applications at the URL and other Canadian crystalline rock research sites are given by Davison and others (1982), Keys (1984), Paillet and Hess (1986, 1987), and Hillary and Hayles (1985). Hearst and Nelson (1985) and Keys (1979) give general reviews of geophysical logging techniques applicable to fractured-igneous and metamorphic crystalline rocks. Anderson and O'Malley (1985), Paillet (1985), and Aguilera (1979) discuss fracture interpretation methods applicable to a much larger range of rock types, including both clastic sedimentary and crystalline rocks; many of these methods can be applied to the geophysical-log data obtained at the URL. These extensive results indicate that the qualitative interpretation of fractures based on conventional geophysical-logging techniques can be conducted in a routine manner by using many established guidelines. The most important issue in such qualitative-interpretation methods is the need for multiple geophysical logs to eliminate ambiguous log responses.

PURPOSE AND SCOPE

The primary purpose of this report is to describe the application of new geophysical measurement techniques and new data processing procedures designed to provide quantitative measurements of fracture permeability and other crystalline rock properties. The approach to log interpretation at the

URL is broken into two distinct parts: (1) Identification and characterization of zones of fracture permeability that form ground-water conduits intersecting the borehole; and (2) characterization and verification of the properties of apparently thick, fracture-free intervals, that might serve as repository horizons. Because of this fundamental division of the geophysical-log interpretation process, the boreholes selected for this study include two deep, fully cored boreholes, penetrating rocks with different fracture frequencies. The first (borehole WRA1) intersects multiple fracture intervals to vertical depths larger than 1,000 m. This borehole is ideal for testing methods for fracture-permeability interpretation. The other (borehole URL13) intersects very few fractures according to the core description, and almost all these fractures are concentrated in the upper 100 m. This second borehole is ideal for testing methods for the verification of massive, fracture-free intervals, and the identification of subtle changes in lithology or the presence of sealed fractures, that might be relevant in the prediction of repository performance.

This report begins by surveying the geophysical logs for both boreholes, listing the distribution and extent of qualitative fracture indicators. Much of this preliminary analysis follows established guidelines, although some attempt is made to relate the size and character of various fracture anomalies to the permeability and extent of alteration in fracture zones. Quantitative fracture permeability estimates are based on two advanced techniques: (1) Acoustic tube-wave amplitude logs; and (2) heat-pulse flowmeter measurements of the distribution of vertical flow in the borehole. The lack of extensive alteration in fracture zones and the small diameter of the URL boreholes provided ideal conditions for the interpretation of acoustic tube-wave amplitude logs. Extensive use of this technique is described in this report. The lack of large, naturally-occurring hydraulic-head differences between fracture zones made flowmeter applications much less useful at the URL. Limited flowmeter measurements are described in this report, but no attempt is made to derive permeability estimates on the basis of these data. Flowmeter measurements would give much more useful information if flow in the fracture zones could be induced by pumping. The design and interpretation of such pumping tests, in conjunction with heat-pulse flowmeter measurements of vertical flow in the borehole (Paillet and others, 1987) will be a useful part of future fracture-characterization studies at the URL.

The extensive discussion of fracture permeability estimates derived from acoustic waveform logs is presented in the anticipation that independent information on fracture permeability will be made available. Previous studies (Paillet, 1980, 1983) have shown that fracture permeability and tube-wave attenuation are correlated in fractured crystalline rocks where there is little alteration in fracture zones to cause difficulty in separating attenuation caused by fluid motion in fracture openings from variations in intrinsic rock attenuation. The large number of well-isolated fractures encountered by borehole WRA1 and the lack of intense weathering in fracture zones indicate that the acoustic waveform logs obtained in this borehole provide an excellent opportunity for the comparison of permeability estimates derived from tube-wave analysis with other, more established, permeability estimates.

3

Description of the Study Site

The Underground Research Laboratory is located approximately 10 km east of the town of Lac Dubonnet in Southeastern Manitoba (fig. 1). Numerous deep core holes have been drilled within a 5-km^2 area at the URL, with additional core holes drilled in adjacent areas of the batholith. The URL series of boreholes refers to the URL location, whereas the Whiteshell Nuclear series have been drilled appoximately 10 km to the southwest of the URL, and the Western Research Area series have been drilled at several sites distributed over the southeastern and central regions of the batholith (fig. 1). The only WRA series borehole used in this study, WRA1, is located approximately 5 km west of the URL. In this report all of the URL, WN, and WRA series of boreholes are referred to collectively as the URL boreholes unless otherwise stated.

The two boreholes used for this study are URL13 and WRA1. Both were drilled approximately 20° from the vertical, and penetrated to a true vertical depth of approximately 1,000 m. The two boreholes were cored the full depth, with distributions of apparently natural open and closed fractures as noted in the core description provided to the U.S. Geological Survey by AECL personnel. Borehole diameters are approximately 7.5 cm. Less than 1 m of regolith was removed from the surface at each of the two sites, so that coring began at the surface, and surface casing extended no more than a few meters into bedrock. All depths given in this report refer to linear distance in meters along the deviated borehole below land surface, as determined by the measuring system incorporated into the U.S. Geological Survey logging equipment. Other data provided by AECL personnel have been subjected to slight adjustments (depth-scale alignment) to make these data consistent with the U.S. Geological Survey depth scale. Photographs of the U.S. Geological Survey logging truck at the URL13 site and a typical small mafic xenolith exposed in outcrop near borehole WRA1 are shown in figure 2. Lithology variations related to the presence of such xenoliths, mostly at shallow depths, and biotite rich and pegmatitic dikes at larger depths, represent the only departures from the homogeneous granitic rocks of the batholith indicated in figure 1.

Geophysical Logging Equipment Used For This Study

All of the conventional geophysical well logging measurements described in this report (caliper, single-point resistance, epithermal neutron, etc.) are described in detail in the literature, and they will not be discussed here. Excellent descriptions of these conventional logs are given by Keys and MacCary (1971), Davison and others (1982), Keys (1984), and Hillary and Hayles (1985). One of the most complete references for all conventional geophysical log measurements, with a discussion of the application of most of these logs to fractured crystalline rocks, is Hearst and Nelson (1985).
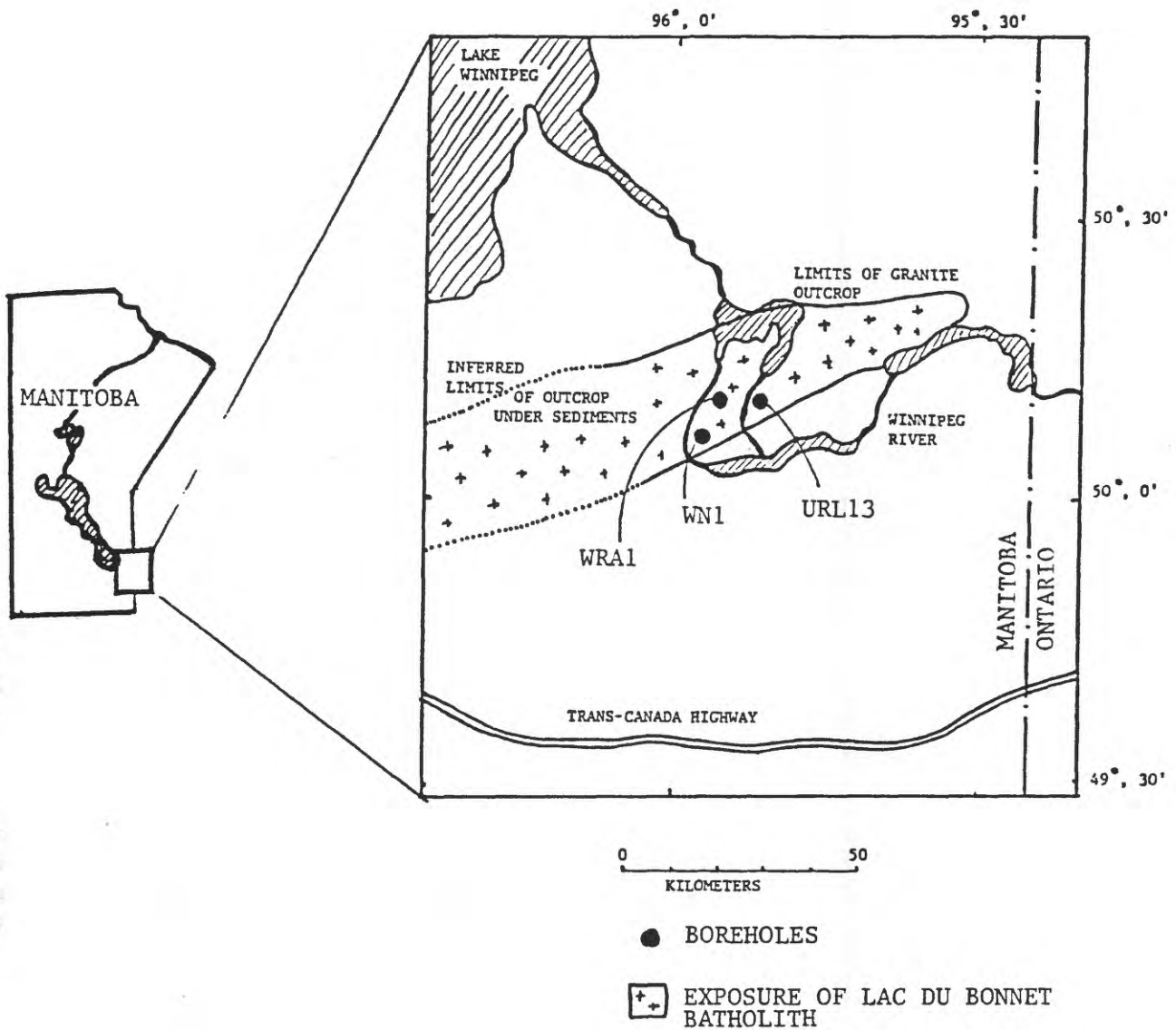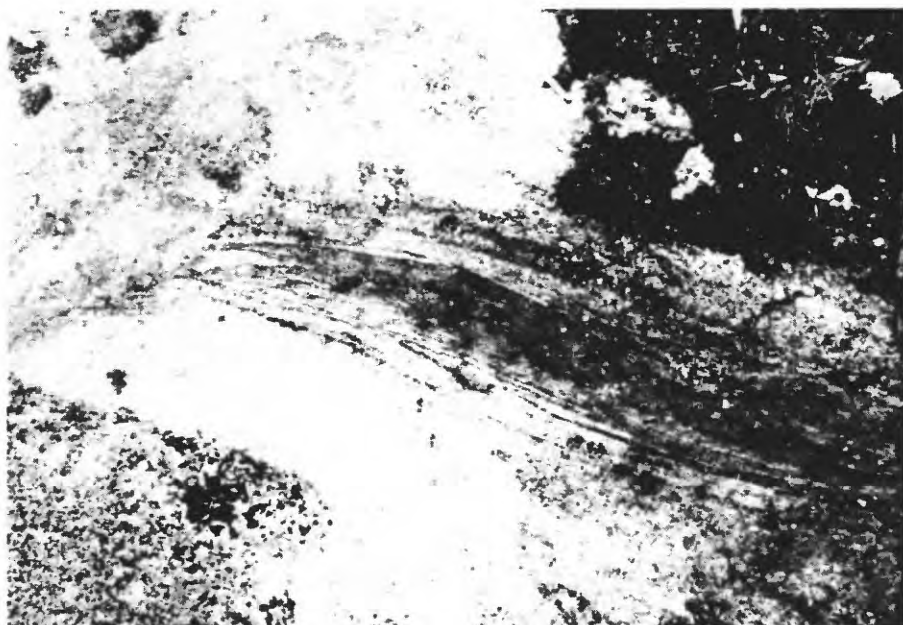
Figure 1.--Location of boreholes URL13, WN1, and WRA1 with respect to
the surface exposure of the Lac du Bonnet Batholith.

5

```
0                        30
        CENTIMETERS
```

Figure 2.--Photographs illustrating A) the U.S. Geological Survey
   logging truck at borehole URL13; and B) appearance of a typical
   small xenolith exposed in granite outcrop adjacent to borehole
   WRA1.

6

The borehole acoustic televiewer (hereafter denoted as the televiewer) was used as the primary means for confirming the presence of fractures indicated on other geophysical logs. The televiewer provides a photographic image of the pattern of acoustic reflectivity on the borehole wall. The irregular surface, where a fracture intersects the borehole wall, appears in the photographic image as a line. The shape and vertical extent of the fracture image in the televiewer log can be used to determine fracture strike and dip, with respect to the borehole axis. Numerical methods for calculating true strike and dip from apparent strike and dip and known borehole deviation are given by Kierstein (1983), and Lau (1983). Zemanek and others (1969), and Keys (1979) describe televiewer log instrumentation and interpretation in more detail. Paillet and others (1985) provide several examples of televiewer-logs compared to core photographs and other fracture data; they also discuss televiewer log interpretation in various lithologies.

The small borehole diameter and deviation of the URL borehole made the application of televiewer logs particularly difficult in this study. Conventional bow-spring centralizers would not work in a deviated borehole because gravitational forces would decentralize the televiewer. This problem especially is severe in small-diameter boreholes because the televiewer would come so close to the borehole wall that reflected acoustic energy would merge with the outgoing signal. These problems were corrected by building up ridges of electrical tape on the outside of the logging-tool body, above and below the source transducer window. These ridges kept the televiewer nearly centralized, but they also increased frictional forces that were opposing lowering the televiewer probe. Slight decreases in borehole diameter with depth, compounded by increasing deviation from the vertical, made the lower parts of borehole WRA1 very difficult to reach. These decreases also prevented logging below depths of 300 m in borehole URL13.

The most extensive use for the quantitative estimation of fracture permeability is based on the interpretation of acoustic waveform logs in which the full-pressure response at the recievers of a conventional acoustic transit-time logging probe is recorded digitally. An acoustic-logging probe was used with a 34-kHz source, and digitized waveforms using a 1-μs sampling rate at 0.15-m intervals along the borehole. The logging probe configuration is described by Paillet (1980, 1983). Limited data also were obtained, using a new, low-frequency sparker source operating at a frequency near 5 kHz (Paillet, 1984). Fracture-permeability interpretation is based on the calculated attenuation of tube waves between an acoustic-probe source and a receiver. Details of the calculation are given in a subsequent section of this report.

Measurements of the vertical flow distribution in the URL boreholes were made using a new, highly sensitive, heat-pulse flowmeter. The flowmeter operates by measuring the time required for the heat pulse introduced at a wire grid to travel approximately 2 cm up or down the borehole (Hess, 1982, 1986). Accuracy of the flowmeter depends upon the width of the annulus between the flowmeter measurement section and the borehole wall. If the annulus exceeds more than a few millimeter in width, flowmeter accuracy is greatly reduced. To improve flowmeter performance, an inflatable packer was installed to block the annulus during the measurement. Preliminary tests indicated that the flowmeter with packer could provide measurements less than 0.01 L/min. However, the

packer system designed for the small-diameter boreholes at the URL failed at
the beginning of the on site work for this study. Therefore, flow measurements
were made with a flowmeter model, with a measurement section nearly filling the
7.5-cm diameter borehole (measurement-section diameter 5 cm), but with a small
open annulus still present. This limitation severely affected the ability to
measure the small values of natural flow present in borehole WRA1. Additional
details on the application and interpretation of heat-pulse flowmeter data are
given by Hess (1986), Paillet and Hess (1986, 1987), and Paillet and others
(1986, 1987).

CORRELATION OF GEOPHYSICAL LOGS

The epithermal neutron, acoustic transit-time, and single-point resistance
logs for boreholes URL13 and WRA1 are given in figures 3 and 4. Keys (1979,
1984), Paillet and Hess (1986) Paillet and others (1987), Hillary and Hayles
(1985), and Nelson and others (1983) describe the qualitative relationship
between fractures and expected anomalies on these logs. The acoustic
transit-time log for the deeper portions of borehole URL13 especially appears
uniform, indicating homogeneous mechanical properties corresponding to a
compressional velocity near 5.8 km/s through this part of the borehole. The
core fracture distribution for the lower part of borehole URL13 indicates very
few closed fractures, and no open, apparently permeable fractures in the
interval from 100 to 1,100 m in depth. A few fractures are indicated on the
core log from 1,100 to 1,200 m in depth, but borehole conditions did not permit
logging below 1,100 m in depth. Most of the anomalies appearing on the three
logs in figure 3 correlate with the few closed fractures detected in core
samples recovered from borehole URL13. The one important exception is the
single, isolated, epithermal-neutron log anomaly at a depth of about 914 m.
This feature does not correlate with any identified core fracture or lithologic
contact. No significant anomalies occur on either the acoustic transit-time or
single-point resistance logs at this depth.

The three logs in figure 4 show numerous anomalies associated with
several major fracture zones, and other isolated fractures indicated on the
core fracture distribution in borehole WRA1. Inspection of the neutron log
indicates major fracture zones in the depth intervals 0-300, 700-800, and
1,140-1,180 m with prominent isolated fractures at 675 and 1,090 m in depth.
Previous results (Keys, 1979, 1984; Paillet and Hess, 1986, Paillet and
others, 1987) indicate that much of this response is attributed to fracture
opening near the borehole and alteration of feldspars to clay in the vicinity
of fractures. Inspection of the acoustic transit-time log for borehole WRA1
indicates that individual acoustic anomalies are isolated even in the three
major-fracture zones. This response indicates that alteration probably is
confined to the immediate vicinity of individual fractures sets, rather than
extending throughout entire fracture zones. If this indication is true, then
acoustic waveform-log analysis (tube-wave amplitude attenuation) especially
will be useful in fracture characterization because attenuation related to
fracture permeability will not be confused with major changes in seismic
velocities and attenuation in the surrounding rocks.

The single-point resistance log for borehole WRA1 in figure 4 indicates
substantial drift and a pronounced oscillation below depths of a few hundred
meters. This drift is attributed to changes in water quality with depth in the
recently drilled borehole. Recharge of fresh water from the upper fracture
zone and the settling of suspended clay in the borehole probably accounted for
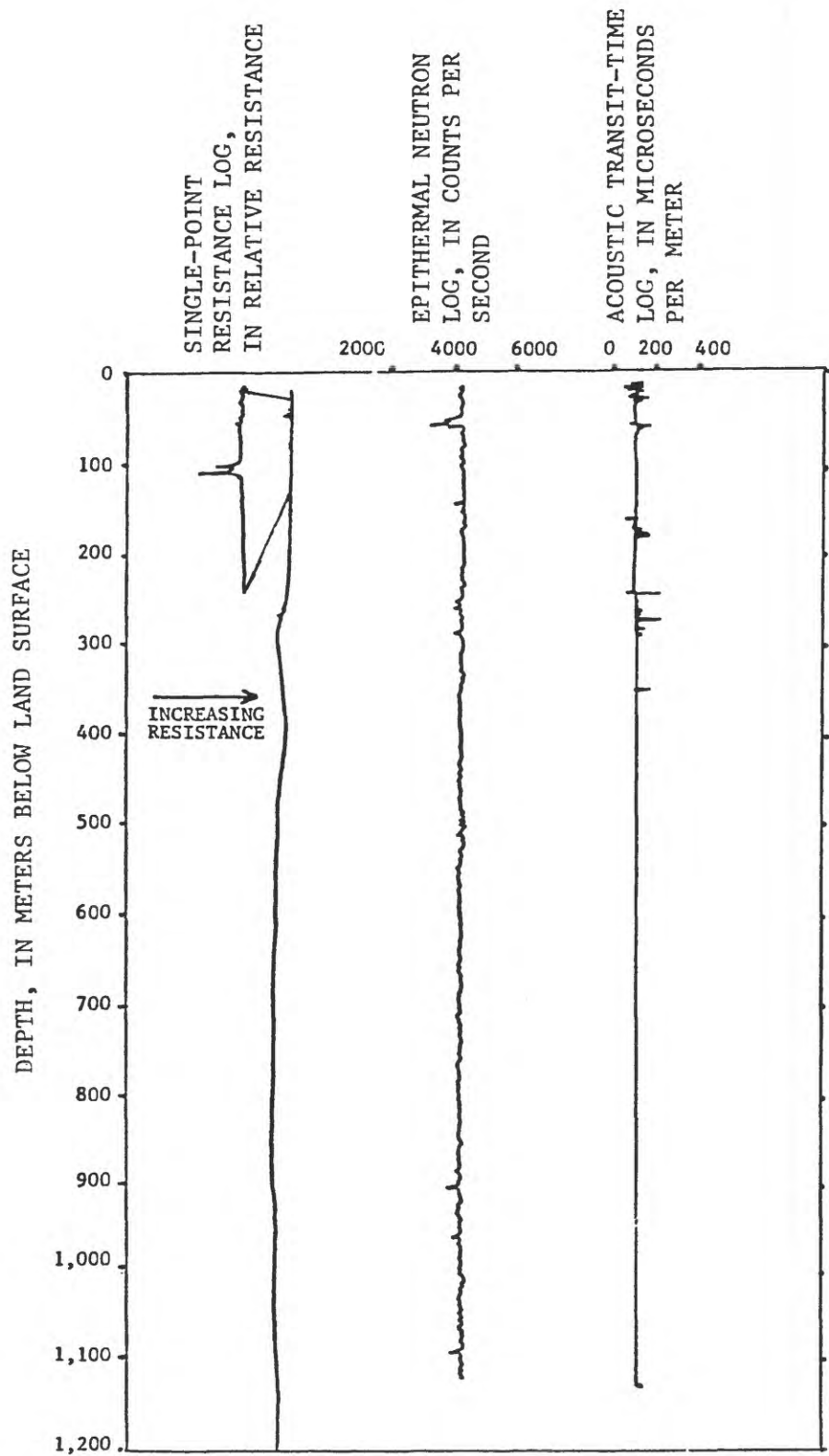
Figure 3.--Composite of epithermal-neutron, acoustic transit-time, and single-point resistance logs for borehole URL13.
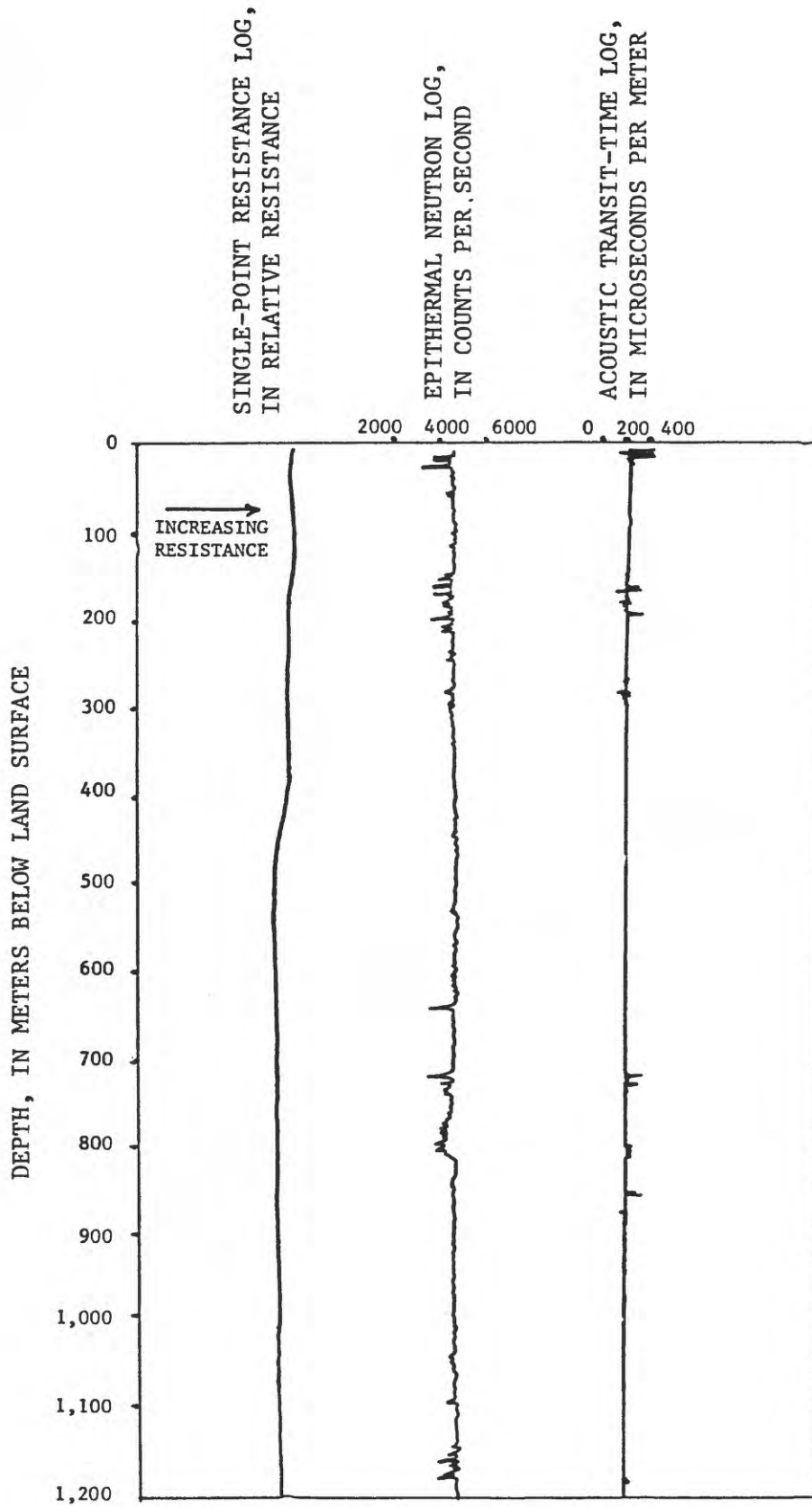
Figure 4.--Composite of epithermal-neutron, acoustic transit-time, and single-point resistance logs for borehole WRA1.

decrease in resistance with depth. The oscillation is attributed to
ectrical interference from an adjacent high-tension transmission line.
nsiderable experimentation with controlling the electrical loading in the
S. Geological Survey logging truck indicated that the frequency of the
scillation could be changed; however, it was impossible to determine a
ombination of conditions that would significantly reduce the oscillation.

Acoustic-televiewer logs in borehole WRA1 indicate discontinuous intervals
of borehole wall breakout in the interval 700 to 800 m deep (fig. 5). These
breakouts appear very similar to extensive breakouts described in basalt flows
in the Pacific Northwest by Paillet and Kim (1987). The generation of such
breakouts is attributed to nonequal horizontal principle stresses, with the
breakouts centered on the direction of minimum stress (Gough and Bell, 1982;
Zoback and others, 1985). The location of the breakouts in figure 5 indicate a
nearly north-south orientation for the maximum horizontal principal stress.
Furthermore, the azimuthal extent of the breakouts in figure 5 indicate that
the ratio of maximum-to-minimum horizontal stress ranges from 1.5 to 2.0:1,
according to the theory of Zoback and others (1985). The relatively limited
extent of breakouts encountered in borehole WRA1, and the lack of breakouts in
other URL boreholes, may indicate that horizontal stresses have been
concentrated in the upper-fracture zones in borehole WRA1, or that alteration
in this fracture zone may have reduced the shear strength of the rock,
permitting breakout formation at lower horizontal stress ratios than those
encountered by Paillet and Kim (1987).

FRACTURE CHARACTERIZATION

Inspection of the geophysical logs in figures 3 and 4 and comparison with
the core fracture distributions provided by AECL shows that the neutron,
acoustic transit-time, and single-point resistance logs indicate the location
and extent of fracturing. One relevant factor in the effectiveness of these
logs in fracture identification is the unusually homogenous lithology of the
granite batholith at the URL. In many other cases, variations in lithology,
vein fillings, contacts, and foliation would produce variations in geophysical
measurements that are unrelated to the presence of fractures, but that may
resemble typical fracture anomalies (Paillet and Hess, 1986; Hillary and
Hayles, 1985). Most applications in fracture characterization related to
repository investigations likely would involve rock masses with relatively
uniform properties, little weathering, and a small frequency of fracturing. In
that case, separation of log anomalies related to lithology from those related
to fractures would be relatively simple in comparison with the more difficult
task of identifying fracture responses against a background of continuously
varying lithology.

The close correspondence between fracture-density and neutron-log
deflections is illustrated in figure 6, showing the correlation between
anomalies on the neutron log and fractures indicated in the televiewer log for
the interval in borehole WRA1 from 130 to 210 m. Similar correspondence
between neutron log deflection and fracture frequency was noted for the two
deeper fracture zones in this borehole; however televiewer-log quality is not
nearly as good at these depths, because of centralization problems and the
increasing deviation of the borehole with depth.

TELEVIEWER LOG INTERPRETATION

720

BREAKOUTS

730

ACOUSTIC TELEVIEWER LOG

DARK STRIP WITH NO DATA CAUSED BY
DECENTRALIZATION OF ACOUSTIC TELEVIEWER
IN SMALL-DIAMETER BOREHOLE

755

756

BREAKOUTS

740

757

DEPTH, IN METERS BELOW LAND SURFACE

758

750

759

BREAKOUTS

BREAKOUTS

760

BREAKOUTS

760

770
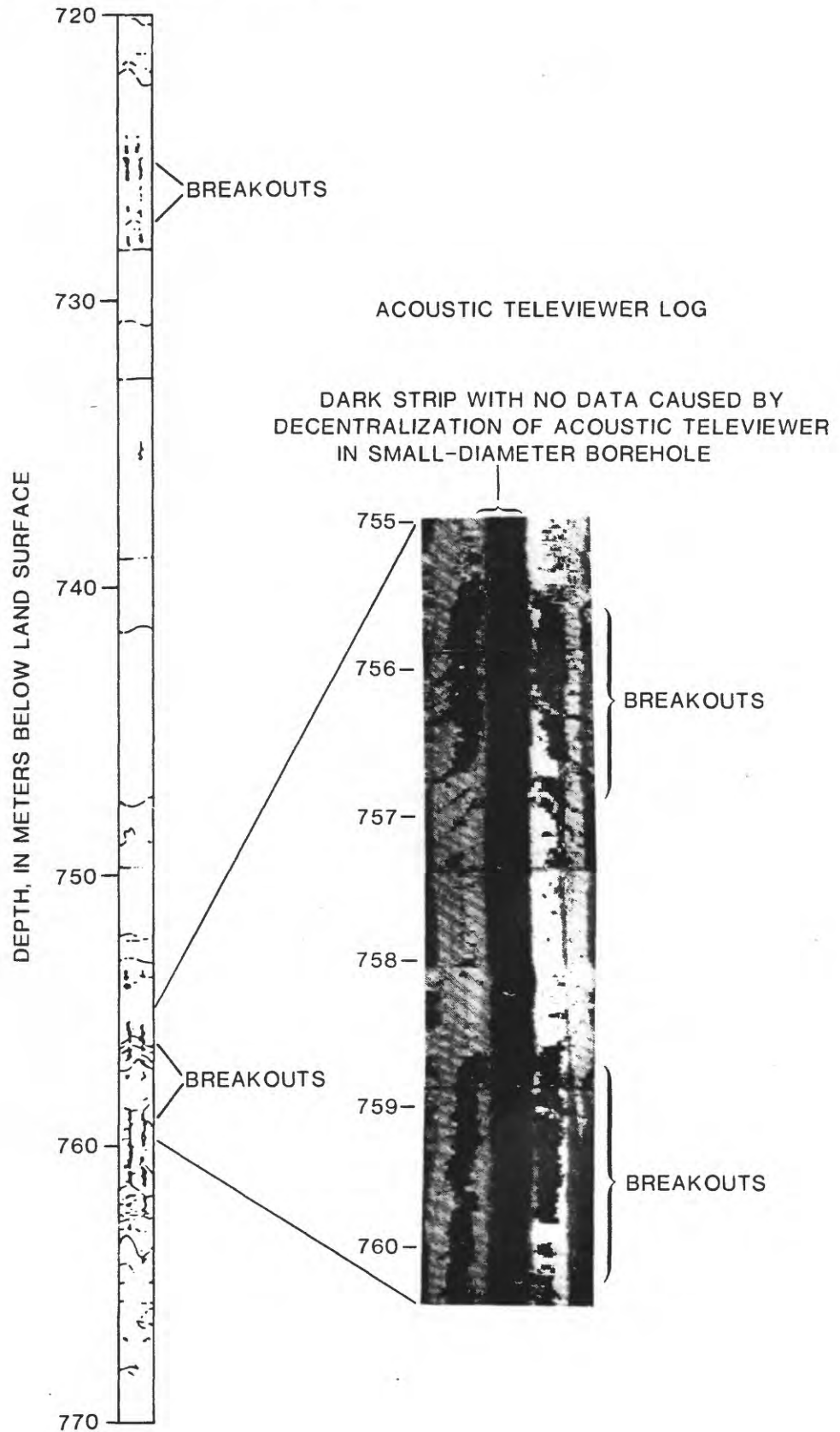
Figure 5.--Borehole wall breakouts indicated on the acoustic televiewer
log obtained in borehole WRA1.

12

EPITHERMAL NEUTRON LOG, IN COUNTS PER SECOND

ACOUSTIC TUBE-WAVE AMPLITUDE, IN PERCENT

TELEVIEWER LOG INTERPRETATION

EXPLANATION

TELEVIEWER LOG INTERPRETATION

ISOLATED FRACTURE

MULTIPLE INTERSECTING FRACTURES

ISOLATED MAJOR FRACTURE

DISCONTINUOUS FRACTURES: PROBABLY OPENED BY DRILLING

DEPTH, IN METERS BELOW LAND SURFACE

Figure 6.--Comparison of neutron log with tube-wave amplitude from acoustic full-waveform log data and acoustic-televiewer data from borehole WRA1.

13

The character of the neutron log in figure 6 and an estimation of the relative volume of actual fluid filled voids present in fracture planes, indicates that almost all the deflections correlating with fractures evident in the televiewer log are caused by alteration around fractures, rather than from fracture porosity. For example, many of the fractures in figure 6 might have an equivalent single-fracture aperture in the range of 0.1 to 0.5 mm. If the sample volume associated with the neutron-logging probe is taken as 1 m in diameter, the ratio of the fracture-opening volume to total sample volume for an interval containing several open fractures would be about 0.001, or much less than one-percent porosity. However, clay minerals may have apparent neutron porosity values larger than 30 percent, so that local alteration of feldspars in granite easily could account for neutron log values equivalent to more than 10 percent porosity. The size of the neutron-log anomalies in figure 6 appear to correlate with apparent width of fracture opening and extent of secondary fracturing indicated by the televiewer log.

Low-temperature alteration of feldspars involves the hydrolosis of silicate minerals. Therefore, the presence of alteration around fractures indicates past movement of ground water in these fractures. The association of neutron-log anomalies with fractures in granite provides indirect evidence of permeability, but it probably cannot be related directly to either the hydraulic conductivity or the porosity of individual fracture zones.

Previous studies (Davison and others, 1982; Keys, 1984; Hillary and Hayles, 1985; Paillet and Hess, 1986) have indicated that the single-point resistance log is a very effective fracture indicator in crystalline rocks. Although relatively fresh ground water is a poor electrical conductor, the clay minerals in altered rock around fracture planes do exhibit much larger elec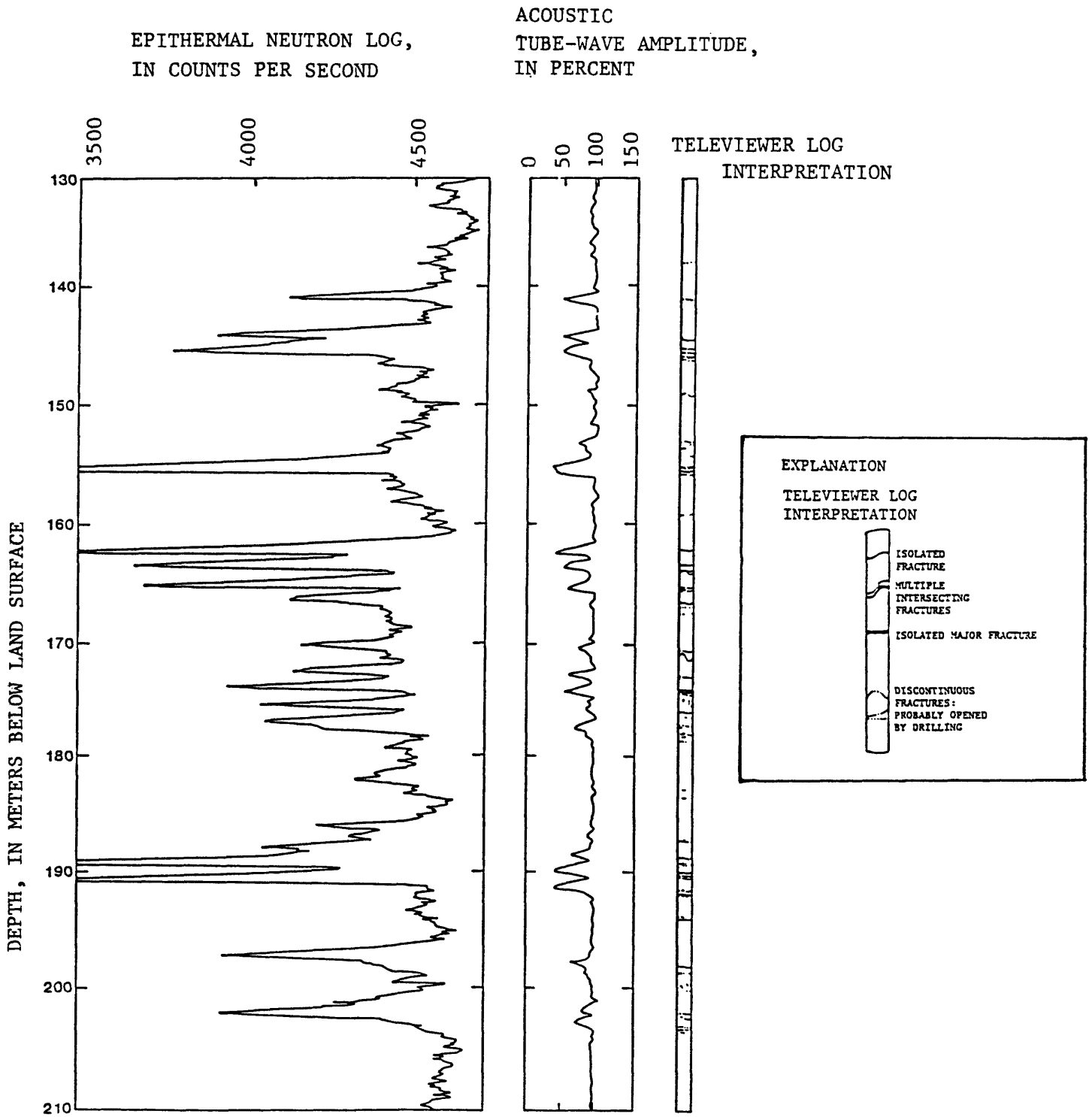trical conductivity values than the highly resistive background. The single-point log especially is useful in identifying these thin conductive zones because the single-point log is not subjected to the anomalous thin-bed effects associated with almost all other more quantitative electric logs (Hearst and Nelson, 1985; Keys and MacCary, 1971). Single-point logs are divided into two slightly different kinds of measurements. The conventional single-point log measures the resistance between an electrode located in the borehole and a surface electrode. The differential single-point log, used by the U.S. Geological Survey in this study, measures the potential difference between two electrodes. Spaced approximately 2 cm apart, the differential single-point log provides somewhat more sensitivity to conditions in the immediate vicinity of the borehole, but it also is more sensitive to minor changes in water quality in the borehole or to slight variations in borehole diameter. Part of the sensitivity of this device to fractures may be caused by slight opening of nearly sealed fractures in the vicinity of the borehole during drilling.

Correlation between single-point log anomalies and fractures in borehole WRA1 is illustrated in figure 7. The single-point log obtained in this borehole was subject to considerable drift and oscillations induced by noise from an overhead transmission line. The single-point log in figure 6 has been modified to remove this drift; it represents a part of the borehole, where

14

SINGLE-POINT RESISTANCE LOG,   TELEVIEWER LOG
IN RELATIVE RESISTANCE   INTERPRETATION
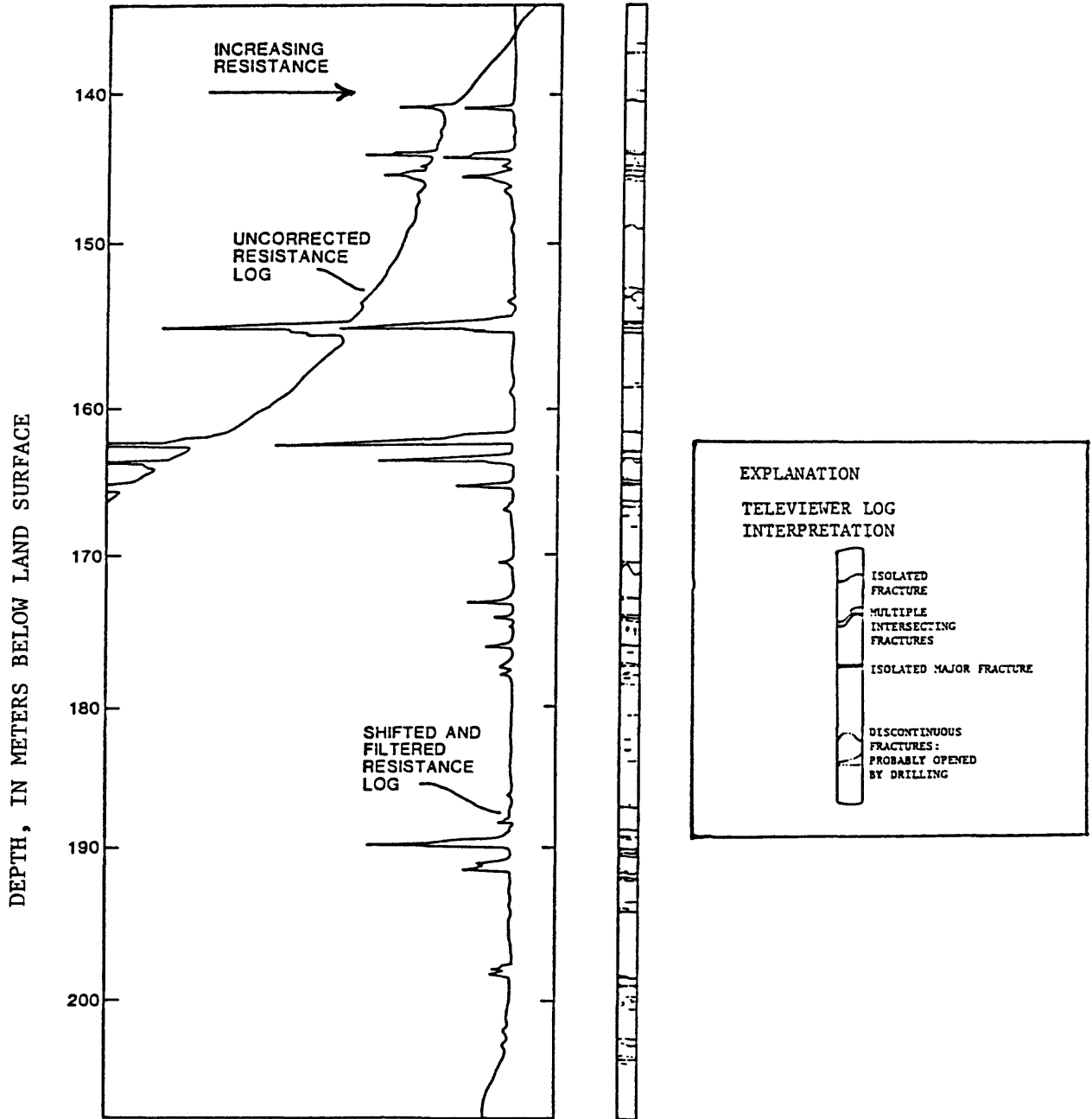

Figure 7.--Comparison of single-point resistance and acoustic-televiewer
    data from borehole WRA1.

noise was not a problem. Removal of drift from the log accentuates the excellent correlation between the single-point log and the televiewer indicators of fracturing. The correlation between resistance and fracturing, as in the case of the neutron log, probably represents an indirect indication of fracture permeability. Here, the electric-log response is attributed to alteration and local widening of the fracture opening at the borehole wall during drilling. The plot of the single-point log for borehole WRA1 in figure 4 indicates one of the major problems with differential single-point logs in comparison with conventional single-point logs. The larger effect of borehole conditions on the differential single-point log may cause these logs to be plotted so that local fracture effects are greatly reduced. The shifted single-point resistance log shown in figure 7 was produced by convolving the original log with a long averaging filter, substracting the filtered log from the original, and increasing resistance scales to amplify fracture anaomalies. Drift removal like that used in figure 7, or other types of data processing may be needed to enhance the fracture response contained in these logs.

UNFRACTURED GRANITE CHARACTERIZATION

Borehole WRA1 was an excellent test hole for identifying zones of fracture permeability. These measurements likely will constitute a critical part of the effort to understand the ground-water hydrology of a rock body that could contain a nuclear waste repository. However, the actual horizon containing the repository will be chosen to avoid such fracture zones, so that in situ characterization of the properties of unfractured rock also will be useful. Borehole URL13 intersects granite with the the smallest frequency of fracturing of almost any borehole in the URL area. The core fracture description provided by AECL indicates no open fractures between 100 and 1,100 m, and a very small frequency of closed fractures below a depth of 300 m. This borehole provided an excellent opportunity to apply geophysical logs to the verification of the small fracture frequency of this rock, and to identify low-amplitude features that may be significant in repository engineering.

The geophysical logs illustrated in figure 3 were searched for indications of anomalies that might be related to fractures. Borehole conditions prevented logging in the fracture zone defined on the core fracture description at depths below 1,100 meters. Potential fracture anomalies were classified according to the fracture index scale given in table 1. The results of this analysis are shown in figure 8; they are summarized in table 2. Large index values indicating large permeability values are associated with the zone of multiple open fractures indicated on the core-fracture summary in the 60- to 70-m depth interval. Some of the logs (especially the single-point resistance and acoustic transit-time logs) indicate large indices for the closed fractures in the 268- to 272-m depth interval on the core-fracture summary. Most of the small index anomalies noted in table 2 at depths below 300 m apparently are associated with isolated, sealed fractures indicated on the core fracture summary. The one major exception is the large, isolated neutron anomaly at a depth of about 914 m associated with a very minor single-point deflection, and no fracture indications on either the core fracture summary or the acoustic transit-time log.
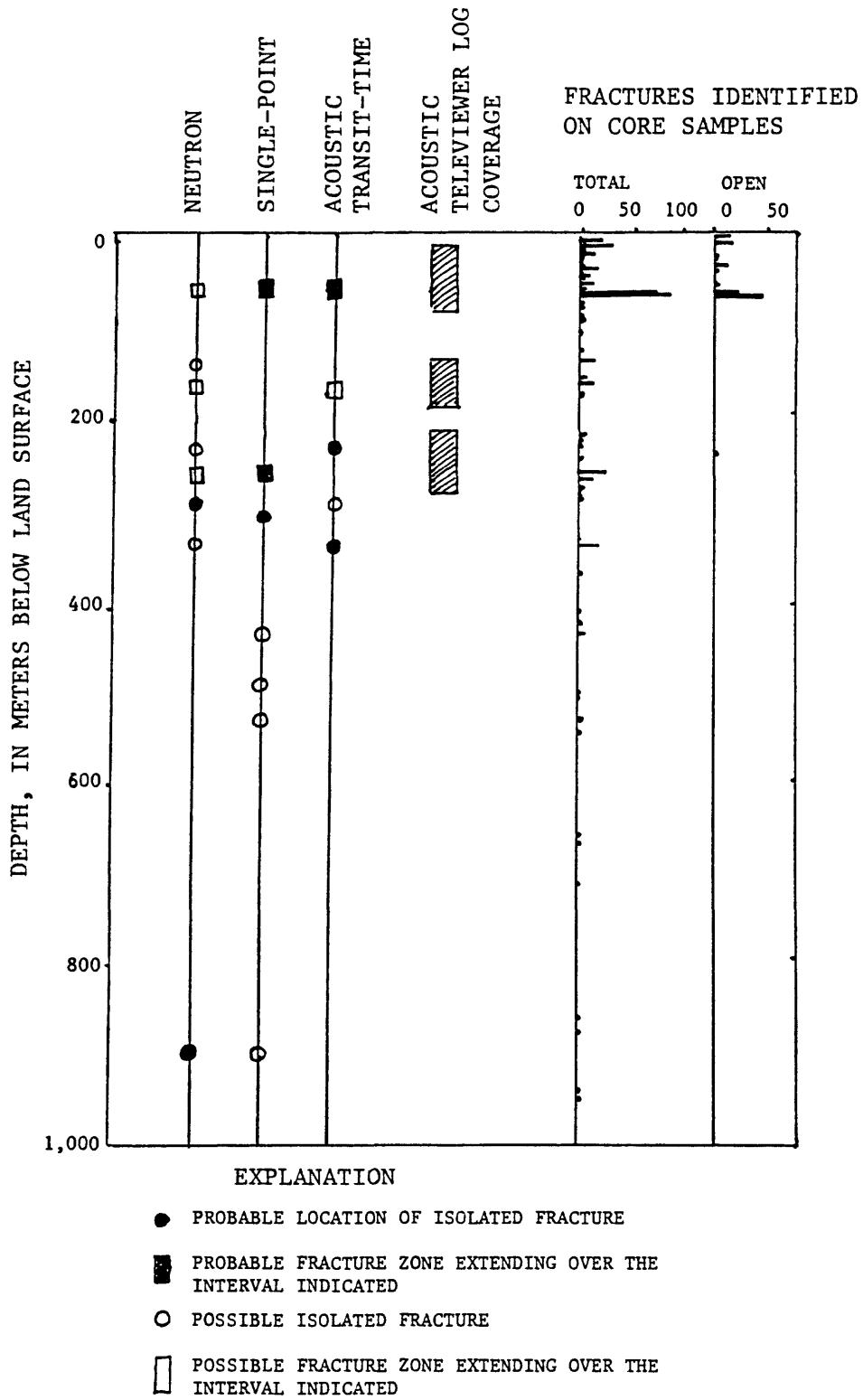
Figure 8.--Summary of fracture indicators on neutron, single-point resistance, and acoustic transit-time logs compared to core-fracture data from borehole URL13.

Table 1.--Fracture anomaly index definition

Index	Definition
0	No possible fracture response indicated.
1	Very minor fracture anomaly indication; would not be considered a possible fracture response if fracture response on other log did not appear to exist.
2	Minor fracture anomaly; would not be considered probable without additional fracture indicators on other logs.
3	Definite but small amplitude fracture anomaly; probable indication of isolated or small set of fractures even without corroborative data.
4	Moderate fracture anomaly; fractures could be permeable; some weathering present.
5	Large fracture anomaly, probably related to multiple, interconnected fractures; fractures considered permeable; considerable weathering in rock adjacent to fractures.
9	Not logged with this device.

Table 2--Fracture anomaly indices in borehole URL13

Depth interval (meters)	Neutron	Single-point	Acoustic	Waveform	Televiewer
60-68	5	4	4	2	5
150	1	0	3	0	1
170-182	1	0	2	0	2
240	1	0	3	0	1
268-272	2	4	4	1	1
297	3	0	1	3	9
312	0	2	0	0	9
346	1	0	3	0	9
442	0	2	0	0	9
486	0	2	0	0	9
544	0	2	0	0	9
590	0	2	0	0	9
914	4	1	0	4	9

Fracture indicators on the various logs were confirmed by televiewer logs in the upper part of the borehole, but centralizer friction in a deviated borehole prevented lowering of the televiewer probe to depths below a few hundred meters. However, acoustic waveform logs were run for the entire depth of the borehole. Inspection of the full waveforms for all possible fractured intervals in figure 8 and table 1 indicated that waveform log anomalies were moderate even in the upper fracture zone in the interval from 60 to 70 m deep. The only significant acoustic-waveform log anomalies were occurred at depths of 297 and 914 m. The uppermost anomaly was associated with several closed fractures on the core fracture summary. The moderate acoustic waveform anomaly at this depth might be attributed to fracture opening during drilling. However, the acoustic waveform anomaly at a depth of 914 m is quite prominent. Inspection of waveforms obtained in the vicinity of this depth indicates that no other significant decreases occur in the wave amplitude comparable to the anomaly at 914 m in depth. Previous experience (Paillet 1983, 1985b) indicates that tube-wave attenuation of this magnitude usually is associated with open fractures. Inspection of the core recovered from the interval extending from 910 to 915 m in depth indicates that a thin mafic band or dike intersects the borehole át about 914 m in depth. The acoustic impedance contrast between this high density rock and the surrounding granite may account for changes in waveform properties, but it does not appear consistent with the observed reduction in tube-wave amplitude.

QUANTITATIVE ESTIMATES OF FRACTURE PERMEABILITY

Inspection of the logs in figure 3 indicates that the numerous fractures intersecting borehole WRA1 at various depths to nearly 1200 m could provide a useful test of the ability to predict fracture permeability by means of acoustic-waveform log analysis. Borehole WRA1 was drilled immediately prior to the logging performed for this study, so there is no independent information on in situ permeability is available, for comparison with the results from the acoustic waveform analysis. Initial results of the quantitative analysis appeared consistent with previous qualitative analysis of the neutron, single-point, and televiewer logs. The acoustic-permeability data are provided here in anticipation that AECL researchers will perform the packer-isolation and hydraulic tests required to verify the permeability estimates based on acoustic waveform attenuation.

The first semi-quantitative attempts to relate acoustic waveform attenuation to fracture permeability are described by Paillet (1980, 1983) and Paillet and White (1982). Their interpretation method is based on the calculations by Rosenbaum (1974) showing that attenuation in the late, large amplitude part of the waveform could be related to borehole-wall permeability. Rosenbaum (1974) failed to distinguish between the different guided modes of propagation that can comprise that late portion of the waveform data. Cheng and Toksoz (1981) and Paillet and White (1982) indicated that for small borehole diameters or low acoustic frequencies the waveform is dominated by the tube-wave mode, that appears to be more sensitive to permeability than all other modes.

The method used in this report is based on calculation of the mean square amplitude in a gated time window corresponding to the tube-wave part of the waveform. This amplitude information then may be plotted in the form of a tube-wave amplitude log for the borehole. The mean amplitude of the tube wave in unfractured parts of the borehole increases with depth because the efficiency of tube-wave excitation increases as the acoustic source works against increasing hydrostatic loading (Paillet, 1983). The tube-wave amplitude log for a typical fractured interval in borehole WRA1 is compared to a full plot of the acoustic waveforms and the televiewer log in figure 9. Each isolated fracture encountered by the acoustic probe produces a drop in acoustic tube-wave amplitude, where the percent amplitude decrease is proportional to fracture permeability, and the vertical extent of the anomaly is caused by the finite source-receiver separation (0.6 m). The tube-wave amplitude log for the entire borehole is deconvolved into individual steps of attenuation that have been assigned the average attenuation at that depth, and a vertical extent of 0.6 m (corresponding to the source-receiver separation). Examples of this deconvolution are shown in figure 9.

Estimation of fracture permeability is made by calculating the observed attenuation as a percent reduction from the amplitude in adjacent unfractured intervals. This attenuation then may be related to the attenuation produced by an equivalent single fracture located midway between source and receiver. These calculations are given by Mathieu (1984), and have been summarized by Mathieu and Toksoz (1984) and Cheng and others (1987). The tube-wave amplitude attenuation calculations express permeability as the aperture (b) of a single equivalent plane fracture.

The tube-wave amplitude log for borehole WRA1 is given in figure 10. Values for attenuation and equivalent single-fracture permeability, associated with tube-wave amplitude anomalies in figure 10 are listed in table 3. Tube-wave amplitudes for the upper part of borehole URL13 are given in figure 11 and equivalent single-fracture apertures calculated from these amplitude values are listed in table 4.

Most permeability measurements are given in units of hydraulic conductivity (m/s) or intrinsic permeability (cm^2). Direct in situ measurements of hydraulic conductivity require packer isolation of discrete intervals and pressure testing (Davison and others, 1982). However, this form of testing requires that the permeability of the fracture zone is averaged with an arbitrary interval of unfractured rock in the packed-off interval. For this reason, we prefer to express fracture conductivity in the form of transmissivity, the product of fracture permeability and thickness. The aperture of a single fracture can be related to fracture permeability through the formula for the average velocity in a plane, parallel fracture (Snow, 1965):

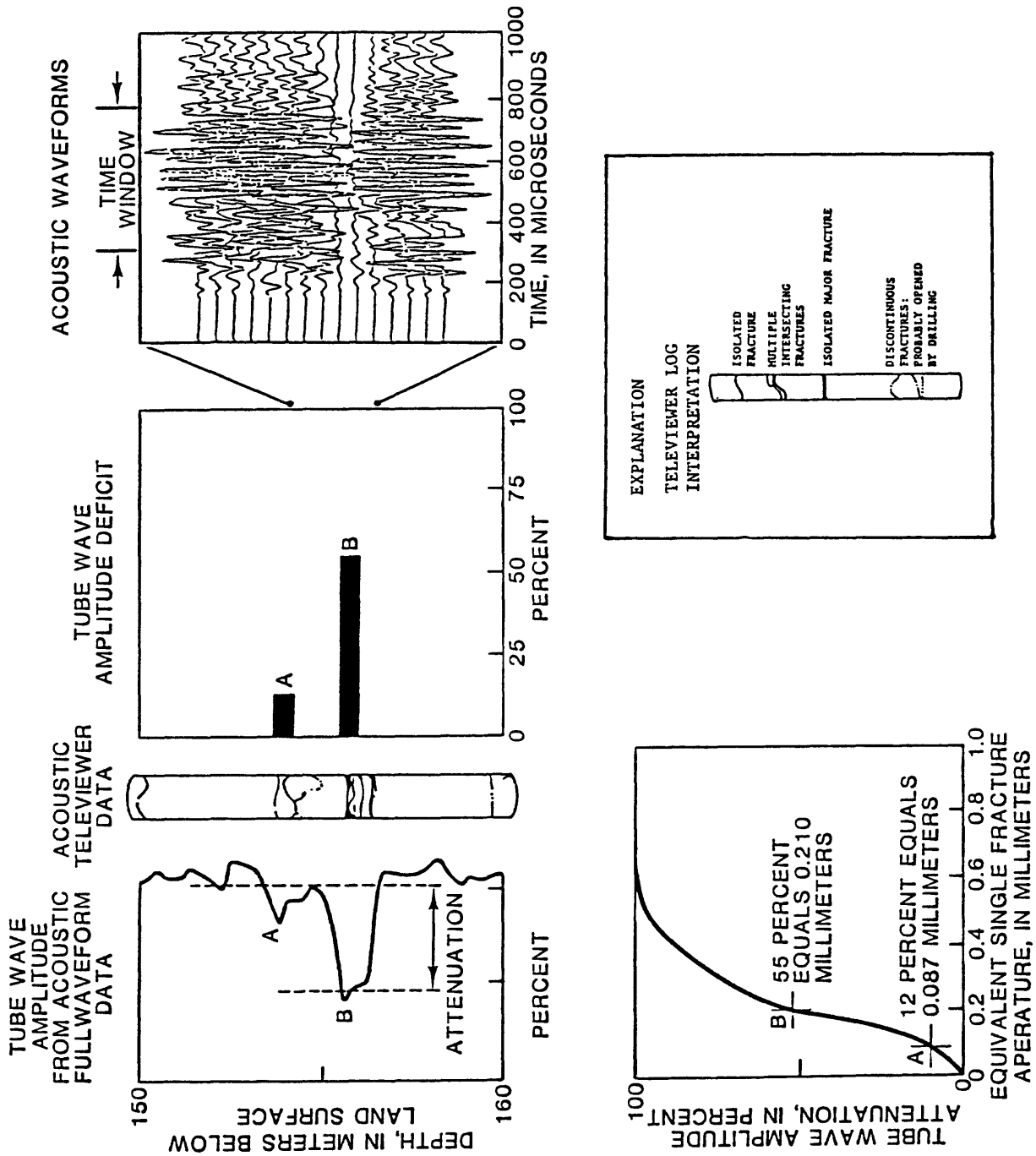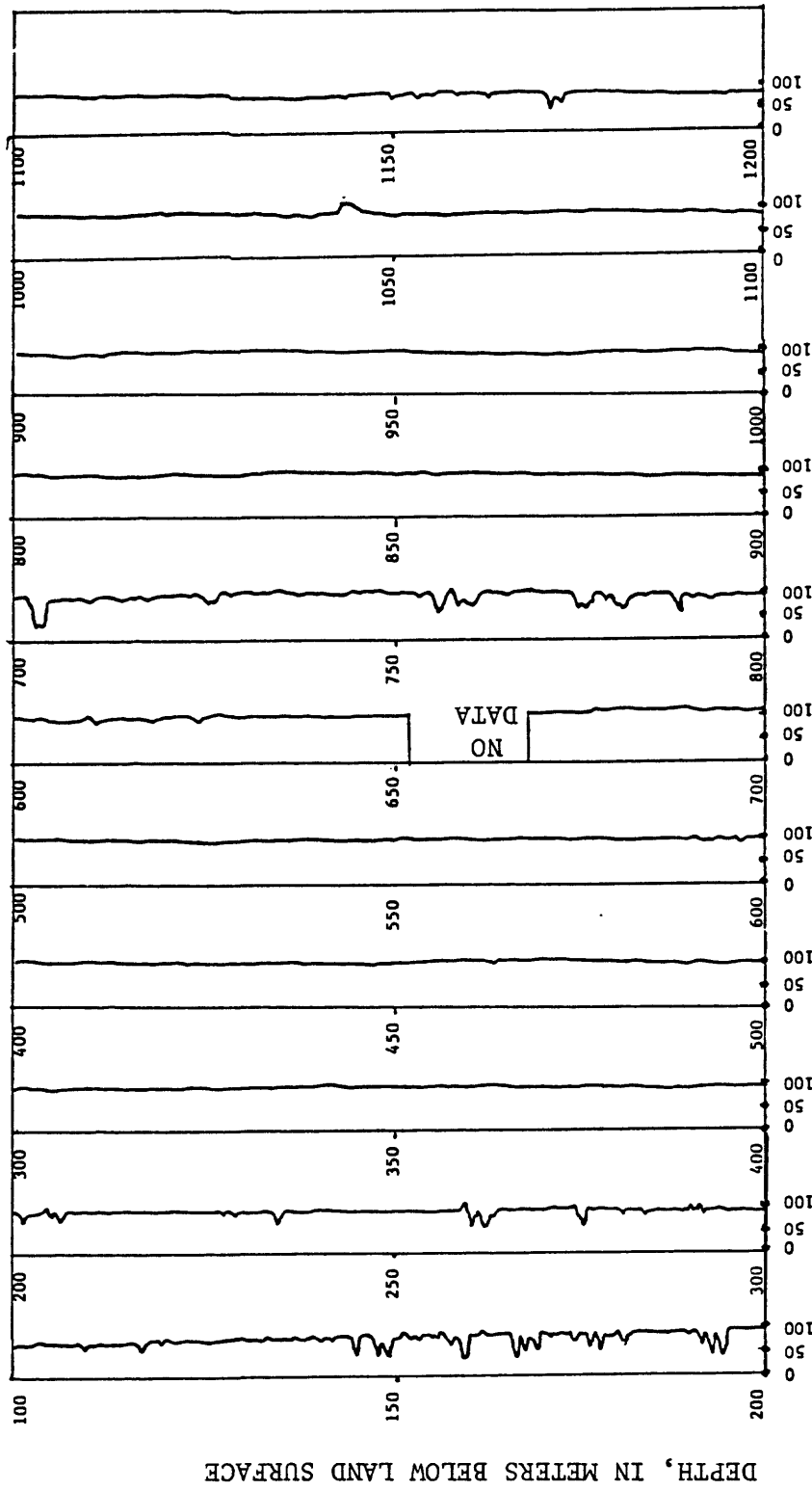$$Q = bv = (\rho g b^2) H'/(12\mu)$$

Figure 9.—Estimation of fracture permeability in equivalent single-fracture aperture, using tube-wave attenuation in acoustic full-waveform data from borehole WRA1.

Figure 10.--Tube-wave amplitude from acoustic full-waveform log data obtained in borehole WRA1.
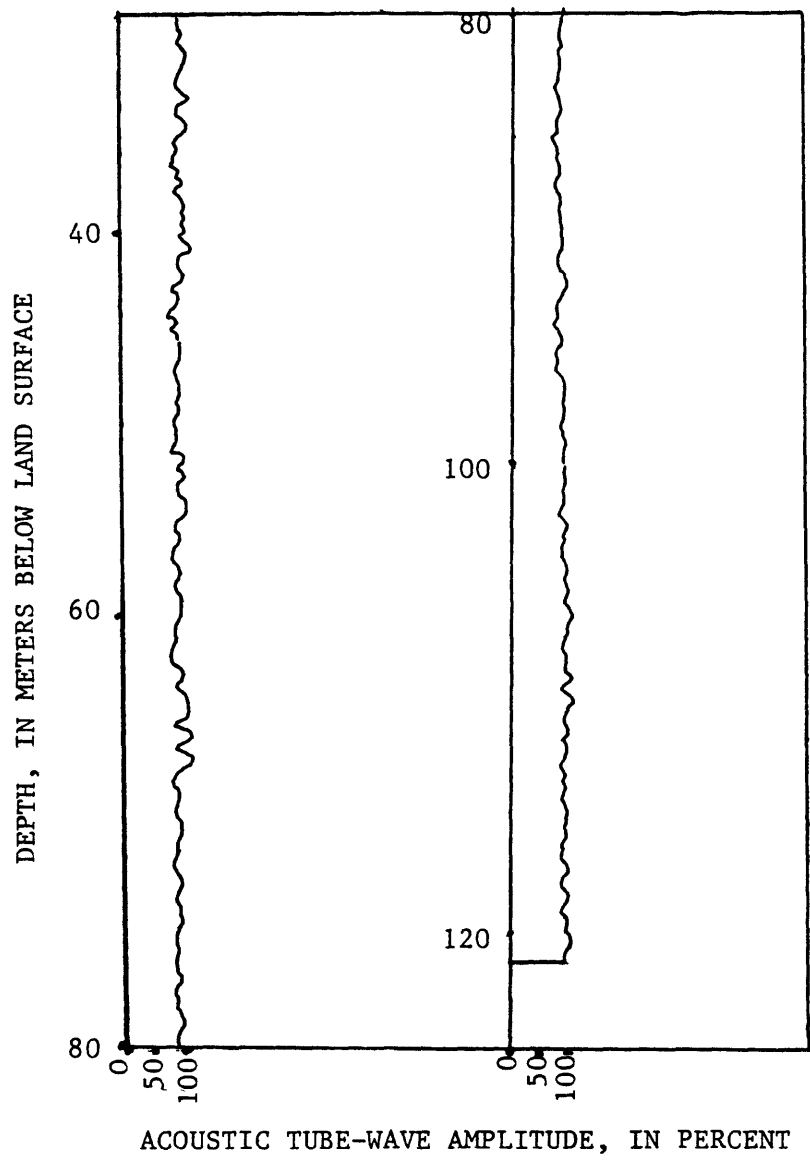
Figure 11.--Tube-wave amplitude from acoustic full-waveform log data obtained in borehole URL13.

Table 3.--Acoustic tube-wave amplitude anomalies identified in borehole WRA1 with equivalent plane fracture apertures and transmissivities [calculated according to Mathieu (1984)]

[m, meter; b - mm, fracture aperature in millimeters; T-cm^2/sec, transmissivity in square centimeters per second]

Depth m	Amplitude deficit (percent)	Aperature (b - mm)	Transmissivity (T-cm^2/sec)	Interval b	T
1,175.61	24	0.13	0.02		
1,174.39	35	0.16	0.04	0.184	0.06
1,165.56	09	0.08	0.005		
1,161.59	06	0.05	0.001	0.086	0.006
1,003.40	10	0.085	0.006		
1,152.14	06	0.05	0.001		
1,145.44	04	0.04	0.000	0.093	0.008
788.52	44	0.18	0.06		
781.81	14	0.10	0.01		
781.20	17	0.11	0.01		
780.59	33	0.15	0.03		
779.68	17	0.11	0.01		
778.15	17	0.11	0.01	0.240	0.140
776.02	22	0.12	0.02		
775.11	33	0.15	0.03		
774.50	33	0.15	0.03	0.203	0.08
761.09	26	0.135	0.025		
760.48	13	0.095	0.009		
759.87	13	0.095	0.009		
759.26	16	0.105	0.012		
757.43	08	0.075	0.004		
756.82	26	0.135	0.025		
756.21	42	0.18	0.06		
754.68	11	0.09	0.007	0.243	0.140
725.73	20	0.115	0.015		
725.12	20	0.115	0.015		
722.68	05	0.045	0.001		
722.07	08	0.075	0.004	0.148	0.03
715.67	08	0.075	0.004		
710.49	05	0.045	0.001		
705.92	05	0.045	0.001		
704.70	08	0.075	0.004		
703.78	60	0.220	0.107		
703.17	60	0.220	0.107		
702.56	60	0.220	0.107	0.315	0.310
626.06	10	0.085	0.006		
625.45	15	0.100	0.010	0.117	0.02

Table 3.--Acoustic tube-wave amplitude anomalies identified
in borehole WRA1 with equivalent plane fracture apertures and transmissivities
[calculated according to Mathieu (1984)]--Continued

Depth m	Amplitude deficit (percent)	Aperature (b - mm)	Transmissivity $(T-cm^2/sec)$	Interval b	T
611.43	15	0.106	0.012	0.100	0.01
596.80	08	0.075	0.004	0.075	0.004
591.62	05	0.045	0.001	0.045	0.001
466.65	08	0.075	0.004	0.075	0.004
291.39	11	0.090	0.007	0.090	0.007
283.16	08	0.075	0.004		
280.11	08	0.075	0.004		
274.62	44	0.180	0.058	0.182	0.06
274.02	33	0.150	0.034		
261.82	14	0.100	0.010		
260.91	39	0.170	0.049		
259.69	17	0.110	0.013		
259.08	33	0.150	0.034	0.239	0.14
232.26	39	0.170	0.049	0.170	0.05
226.47	08	0.075	0.004		
224.94	08	0.075	0.004	0.095	0.009
202.69	24	0.130	0.022		
186.54	17	0.110	0.013	0.152	0.04
197.51	24	0.130	0.022		
190.80	55	0.205	0.086		
189.59	55	0.205	0.086		
188.06	28	0.140	0.027		
186.54	05	0.045	0.001	0.278	0 .21
177.09	22	0.125	0.020		
174.04	35	0.160	0.041		
172.82	32	0.150	0.034		
170.99	18	0.115	0.015	0.218	0.10
166.73	06	0.050	0.001		
165.51	30	0.140	0.027		
163.68	36	0.160	0.041		
162.46	46	0.190	0.069		
155.14	55	0.205	0.086		
153.31	10	0.080	0.005	0.289	0.24
149.05	10	0.080	0.005		
145.69	42	0.180	0.058		
144.48	40	0.170	0.049		
141.43	40	0.170	0.049	0.250	0.16
112.47	18	0.115	0.015	0.115	0.02
104.85	06	0.050	0.001	0.050	0.001

Table 4.--Acoustic tube-wave amplitude anomalies identified in borehole
URL13 with equivalent plane fracture apertures and transmissivities
[calculated according to Mathieu (1984)]
[m, meter; b - mm, fracture aperature in millimeters; $T-cm^2/sec$,
transmissivity in square centimeters per second]

Depth m	Amplitude deficit (percent)	Aperature (b - mm)	Transmissivity ($T-cm^2/sec$)	Interval b	T
47	.10	.085	.006	.085	.001
65	.15	.100	.010	---	---
66	.15	.100	.010	.13	.020
159	.05	.045	.001	.045	.001
240	.05	.085	.006	.085	.006
298	.20	.115	.015	.115	.015
914	.40	.170	.049	.170	.049

where Q = discharge per unit length of fracture,
     b = fracture aperture,
     v = average discharge velocity per unit length of fracture,
     g = acceleration of gravity,
     ρ = density of water,
     H'= hydraulic head gradient driving flow,
     μ = viscosity of water.

Invoking the definition of hydraulic conductivity:

$$T = kb = (\rho g b^3)/(12\mu);$$

where T is the transmissivity of the fracture in square centimeter per second. The transmissivity values of separate fractures are added to give the transmissivity of a single-equivalent fracture. Therefore, the equivalent single-fracture aperture of several adjacent fractures are related by the expression:

$$b^* = (b_1^3 + b_2^3)^{1/3};$$

where b* is equivalent single-fracture aperture conducting the same flow as two adjacent fractures of equivalent single-fracture apertures b_1 and b_2. Additional discussion of the relationship between the permeability of real fractures and equivalent single-fracture aperture is given by Witherspoon and others (1981).

The transmissivity values estimated for fractures indicated by tube-wave amplitude anomalies in figure 10 and 11 are listed in tables 3 and 4. Fracture isolation and injection tests require extensive preparation time, with additional periods for packer seating and pressure testing. The large depths of the URL boreholes probably will require that relatively long intervals be used for this testing in the construction of permeability profiles for the entire borehole. We have combined the transmissivity values listed in table 3 into equivalent transmissivity for 15-m intervals under the assumption that efficient packer testing of borehole WRA1 will require the use of intervals ranging from 10 to 20 m. These results are given in figures 12, 13, and 14. These permeability profiles compare quite favorably with the distribution of apparently open fractures, noted on core fracture summaries given by AECL.

The one major exception to the core fracture data is given by the significant fracture anomaly near a depth of 914 m in borehole URL13. Another smaller anomaly occur at a depth of 297 m in the same borehole. These two acoustic tube-wave amplitude anomalies are compared to a similar anomaly associated with a prominent fracture set indicated on the televiewer log in borehole WRA1 in figure 15. Although no core fracture was noted at 914 m in

28

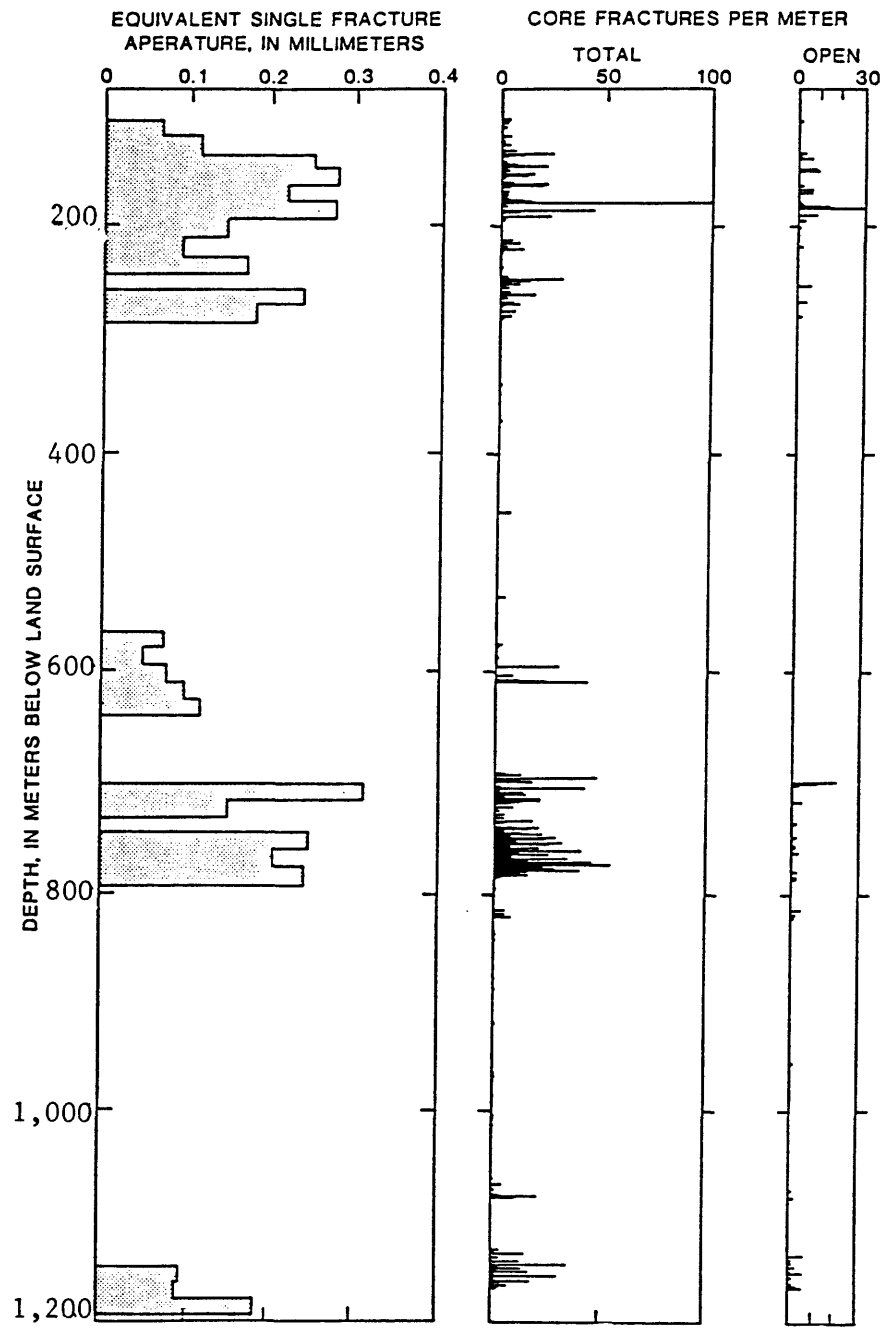Figure 12.--Equivalent single-fracture apertures of fractures within 15-meter intervals in borehole WRA1.
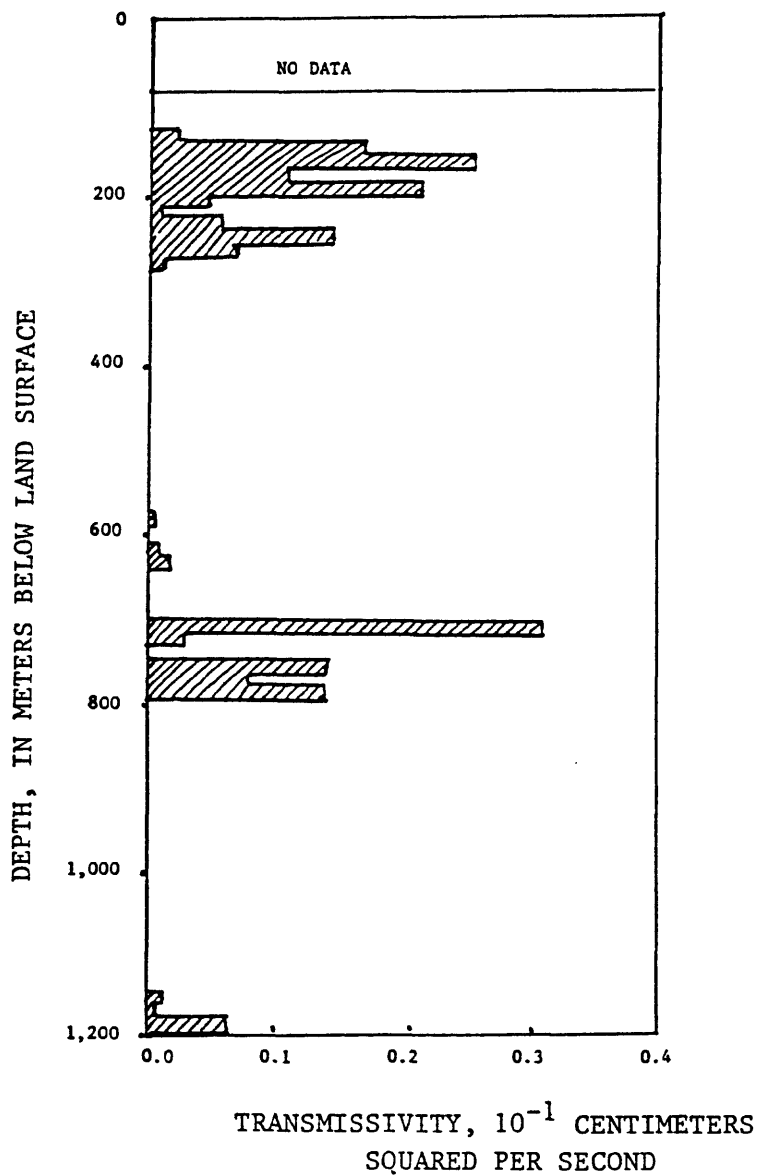
Figure 13.--Effective transmissivities of fractures in
    15-meter intervals in borehole WRA1 estimated using
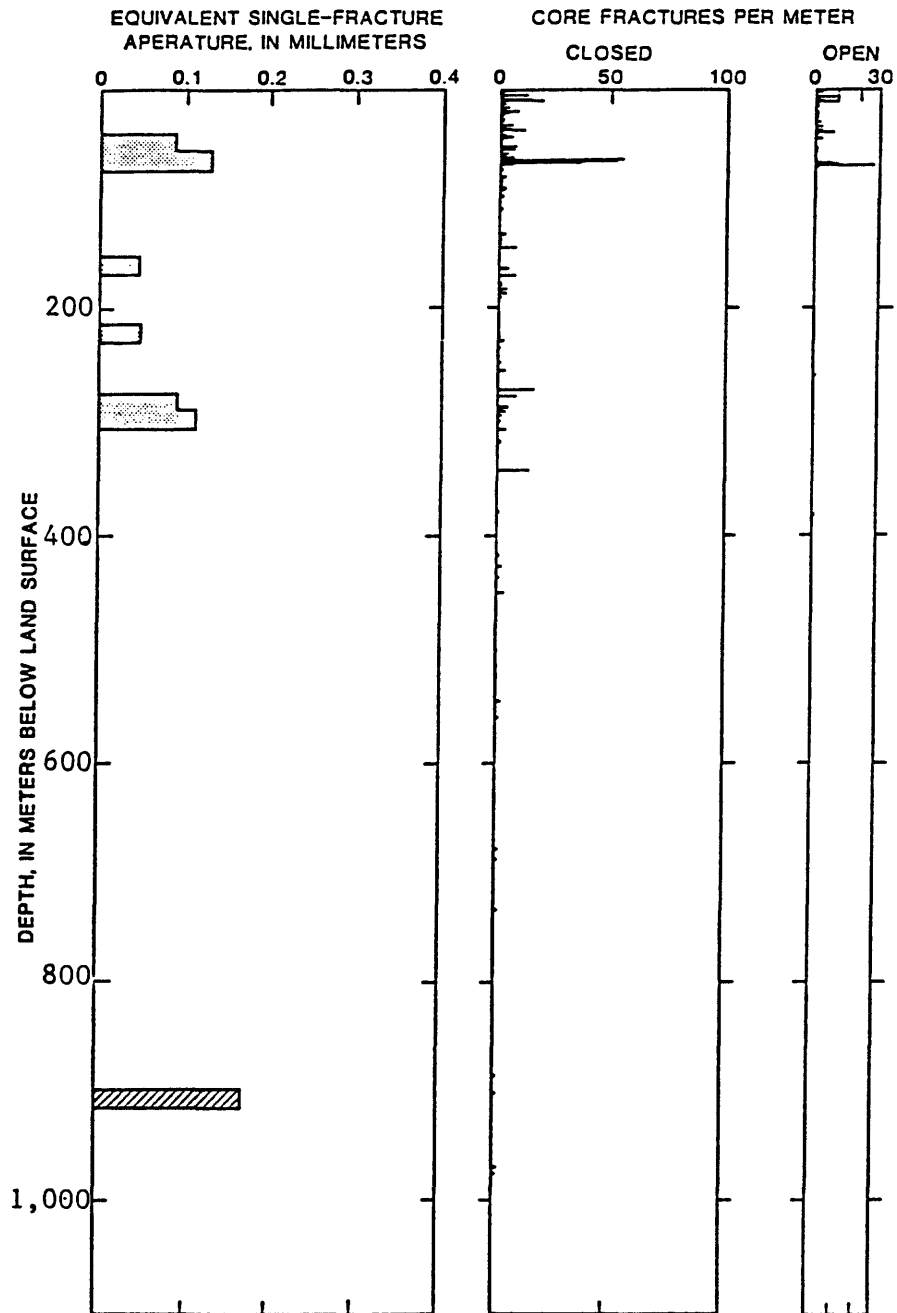   tube-wave attenuation.

Figure 14.--Fracture permeability expressed as effective aperture
in 15-meter intervals interpreted from acoustic tube-wave
attenuation compared to core-fracture data for URL13.

31

borehole UR113, and neither the acoustic transit time nor the single-point resistance logs indicated a significant anomaly at this depth, the tube-wave amplitude anomaly yields an equivalent single-fracture permeability of 0.2 mm or a transmissivity of 0.08 cm^2/s (table 3). The tube-wave attenuation in figure 15b indicates that the attenuation near the depth of 914 m in borehole URL13 resembles attenuation anomalies in borehole WRA1 that clearly are associated with permeable fractures. The neutron log also exhibits a sharp anomaly that resembles some of the fracture anomalies shown in figure 6.

The character of the acoustic waveform anomaly near 914 m in depth in borehole URL13 can be investigated by comparing the acoustic waveforms recorded near that depth in borehole URL13 with waveforms recorded in fractured intervals in borehole WRA1. Results of this comparison are in figure 15. Inspection of the waveforms recorded in the vicinity of 914 m in depth in borehole URL13 indicate that tube-wave amplitudes are much smaller than those recorded in adjacent unfractured intervals. This degree of attenuation appears similar to the attenuation associated with waveforms recorded in borehole WRA1 adjacent to major fractures identified on the acoustic-televiewer log. However, the character of the attenuation near 914 m in depth in borehole URL13 is quite different in detail. The most significant difference is the nearly complete lack of shear-wave attenuation in the lower waveform in figure 15B (waveform D). Previous studies of the effect of fractures on the propagation of acoustic waves in boreholes indicate that shear waves are attenuated even more than tube waves, although the amount of shear-wave attenuation is much more difficult to predict (Paillet, 1980, 1983). The example of tube-wave attenuation at a major fracture zone in borehole WRA1 given in figure 15A (waveform A) illustrates the significant shear attenuation (arrival times ranging from 200 to 300 μs) associated with a measured tube-wave amplitude deficit of approximately the same magnitude as that measured at a depth of 914 m in borehole URL13. The lack of shear-amplitude attenuation in figure 15B (waveform D) indicates that the measured tube-wave attenuation may not be associated with fracture permeability, in spite of the resemblance of this tube-wave amplitude anomaly to anomalies associated with fractures on the acoustic televiewer log for borehole WRA1.

The similarity between the tube-wave amplitude anomalies in figures 15A and 15B raises an important question about the use of tube-wave amplitude data in the estimation of fracture permeability. The tube-wave amplitude deficit evaluated at 914 m in depth in borehole URL13 appears to be related to the lithologic contrast between background granite and a thin mafic intrusion, rather than fracture permeability even though previous studies indicate that tube-wave progation (velocity and amplitude) is very insensitive to even major changes in seismic velocities for hard, crystalline rocks (Paillet and White, 1982; Cheng and Toksoz, 1981). Unusual borehole conditions could have affected tube-wave propagation in the vicinity of the intrusion, but anomalous borehole conditions likely would have produced significant anomalies on the acoustic transit-time and single-point resistance logs. No such anomalies are noted (fig. 8). The only possible cause of the observed tube-wave amplitude observed near 914 m deep in borehole URL13 appears to be amplitude of

MAJOR PERMEABLE FRACTURES IN BOREHOLE WRA1

POSSIBLE FRACTURES IN BOREHOLE URL13

ACOUSTIC
TELEVIEWER
DATA

ACOUSTIC TUBE WAVE
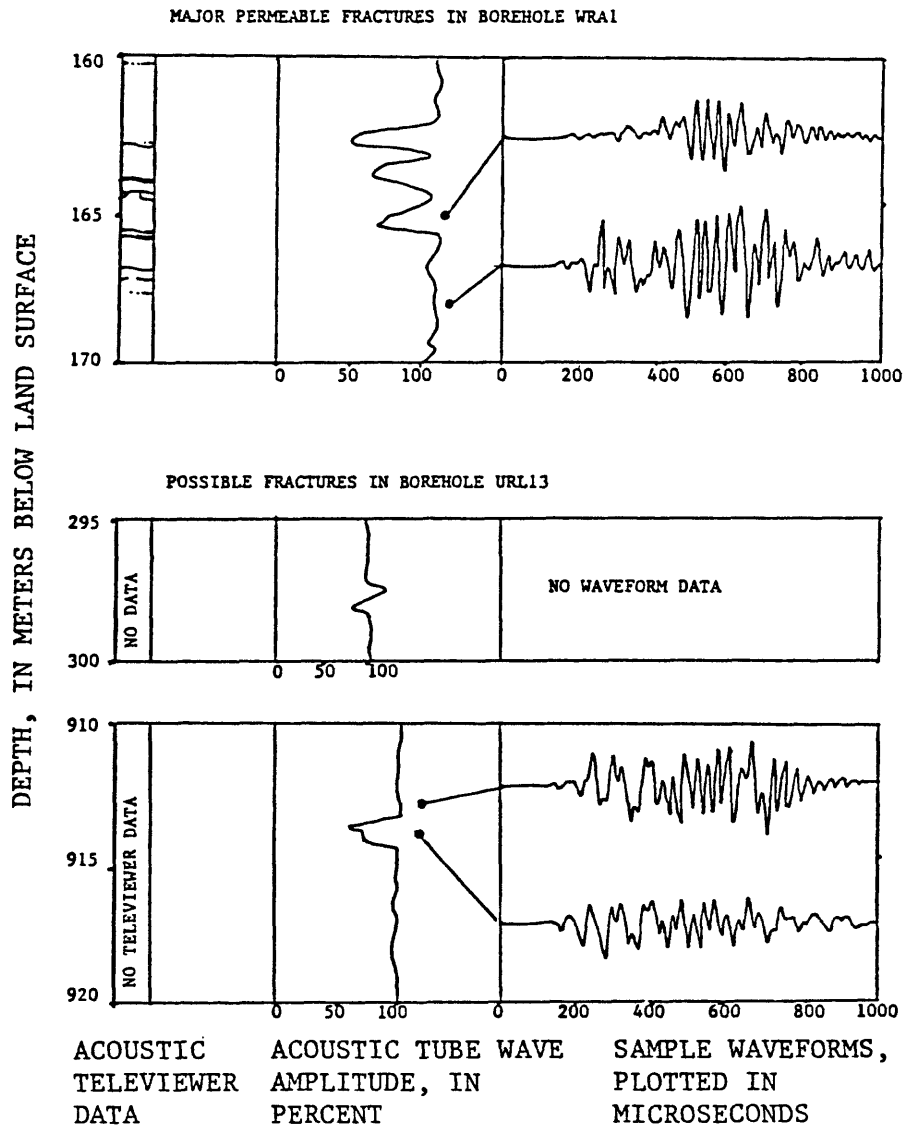AMPLITUDE, IN
PERCENT

SAMPLE WAVEFORMS,
PLOTTED IN
MICROSECONDS

Figure 15.—Comparison of acoustic full-waveform
tube-wave amplitude-log anomalies associated
with identified fractures in borehole WRA1
with similar anomalies associated with suspected
fractures in borehole URL13.

tube-wave excitation in the vicinity of the thin intrusion noted on the core by AECL geoscientists. This unexplained acoustic full waveform log anomaly in borehole URL13 will be the subject of intense investigation, including repeat acoustic waveform logging, acoustic-televiewer logging, and detailed examination of core samples, during future on site equipment testing at the URL.

EXPERIMENTAL TECHNIQUES OF FRACTURE CHARACTERIZATION

Low-Frequency Acoustic Full Waveform Logging

An experimental, low-frequency sparker source has been adapted to work with a conventional acoustic logging system to determine the improvement in acoustic sampling associated with longer seismic wavelengths (Paillet, 1984). The source was developed to provide effective excitation of tube waves in larger diameter boreholes. Sparker source frequencies vary from 4 to 7 kHz for various borehole diameters and depths. The low frequencies are produced by the collapse of a water bubble generated by the sparker discharge, so that sparker source performance deteriorates when the source operates at hydrostatic heads large enough to prevent bubble formation (Paillet and Hess, 1986). For this reason, the sparker source is effective only at depths less than approximately 300 m. The small diameters of boreholes WRA1 and URL13 allow good generation of tube waves at higher frequencies such as those produced by the 34-kHz magnetostrictive source used to obtain most of the acoustic full-waveform logs used for this study. For these small diameters, the low-frequency excitation produced by the sparker source occurs below the optimum-frequency band for tube-wave excitation (Paillet and White, 1982). However, some sparker source data was obtained for this study in an effort to assess the effects of longer acoustic wavelengths (associated with larger sample volumes but less vertical resolution) on acoustic full waveform log interpretation.

Tube-wave amplitude logs generated from full-waveform data obtained with the sparker source are compared to tube-wave amplitude logs generated from full waveform data obtained using the higher frequency magnetostrictive source in figure 16. In previous application of the sparker source, periodic failure to achieve full capacitor discharge produced spurious drops in waveform amplitude that could be interpreted as fracture attenuation. The sparker source was repaired and modified to reduce this problem for this study. The tube-wave amplitude logs illustrated in figure 16B indicate that incomplete discharge was not a problem. However, the data indicate some local increases in amplitude in the depth interval from 178 to 190 m. These anomalous increases in amplitude could be related to some form of resonance in which the longer wavelengths are tuned to the fracture spacing. The recent modifications to the source also may have allowed sparker over-discharge, while preventing the earlier problems with incomplete discharge.

TUBE-WAVE AMPLITUDE DATA
FROM ACOUSTIC FULL-WAVEFORM
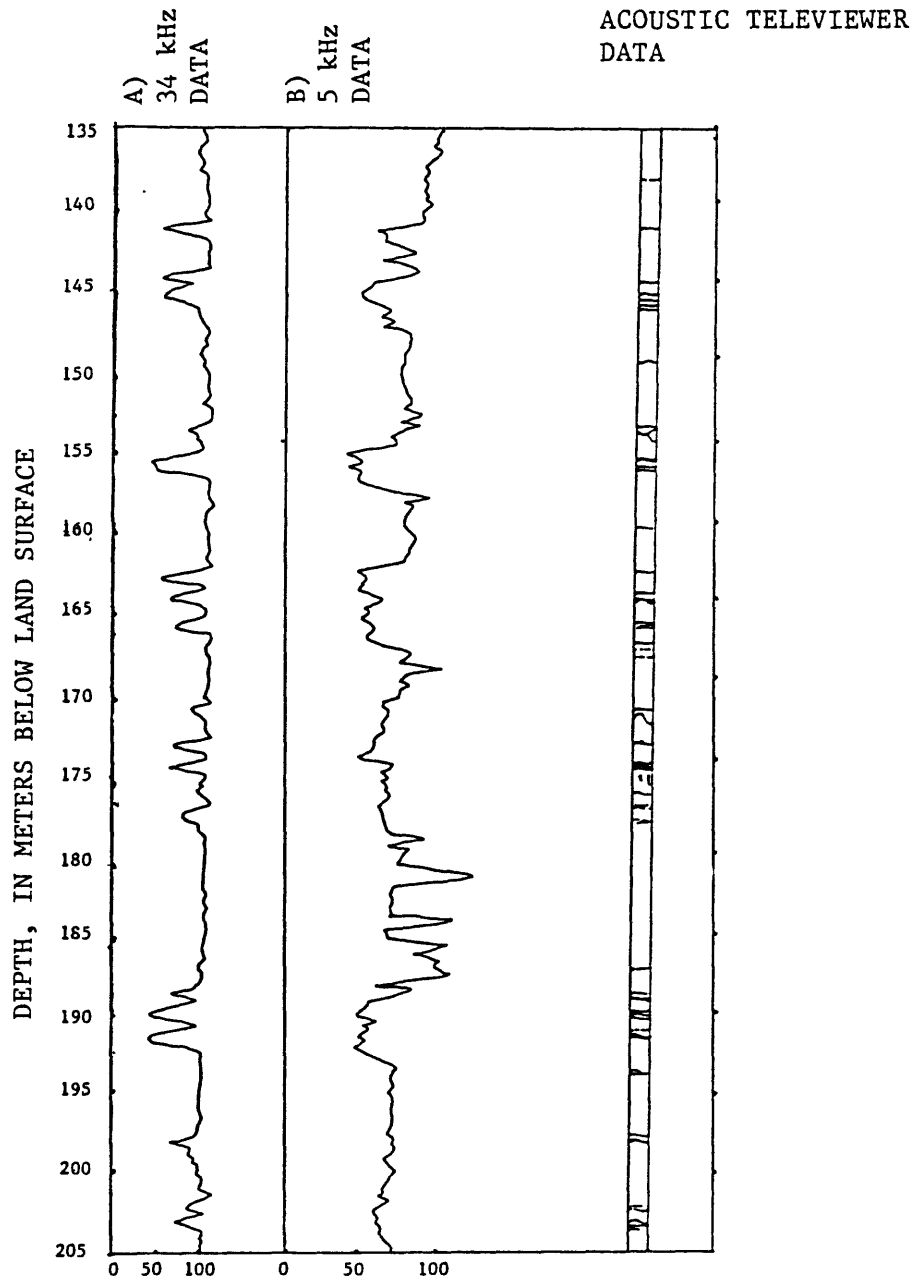LOGS, IN PERCENT OF AVERAGE
AMPLITUDE

Figure 16.--Comparison of tube-wave amplitudes determined
from: A) conventional magnetostrictive acoustic waveforms;
and B) low-frequency sparker waveforms; data from
borehole WRA1.

The longer wavelengths provided by the sparker source produce wider wider tube-wave amplitude anomalies, as illustrated by the example in figure 16. The wider anomalies produce the expected decrease in vertical resolution in that several discrete sets of fractures identified in figure 16A using the higher frequency data, merge into a single broad anomaly in figure 16B, where the lower frequency data have been used. The amplitude reduction associated with the sparker source data in figure 16B also appears somewhat less than that in figure 16A. Part of this effect is attributed to the shift in the fracture permeability curves given by Mathieu (1984) for lower source frequencies; similar fracture permeabilites are associated with smaller amplitude deficits for lower frequencies in the theory. However, the shift between 34 and 5 kHz is not large, so that some of the smaller levels of attenuation in figure 16B may be a sample volume effect. That is, the longer sparker source wavelengths propagate deeper into the borehole wall, sampling more of the fracture plane away from the zone of drilling-induced aperture enlargement.

Another effect associated with longer wavelengths produced by the sparker source is the coherent reflection of low-frequency tube waves off fracture planes. These reflections never have been noted for the higher frequency data, but they have been noted for the sparker data in previous studies. An example of these reflections is given in figure 17. The observed reflection is much larger at the top of the fracture, and the presence of additional fracturing below the main fracture zone apparently disrupts the tube-wave reflection below the fracture zone. The coherent reflections apparently occur at longer wavelengths because small-scale irregularities on fracture-plane surfaces scatter shorter wavelengths, such as those produced by the 34-kHz magnetostrictive source used in this study. Therefore, the independent information provided by these reflections may provide useful additional information about fracture permeability.

Heat-Pulse Flowmeter Measurements of Natural Flow

Resistance to flow through the measurement section of the heat-pulse flowmeter has been found to result in a major limitation on the lower limit of flow resolution for this instrument (Hess, 1986). Recent tests of a wireline-packer system to seal the annulus between the flowmeter and the borehole wall have proven very successful, using a system designed for operation in larger diameter boreholes. This modification was not considered relevant for the operation of the flowmeter at the URL, because most URL boreholes have a diameter (approximately 8 cm) only slightly larger than the measurement section of one of the flowmeters (6.4 cm). A recently-designed version of the packer system was prepared for use in the small diameter boreholes. However, the packer system failed during initial tests, so that only a few very preliminary results were obtained.
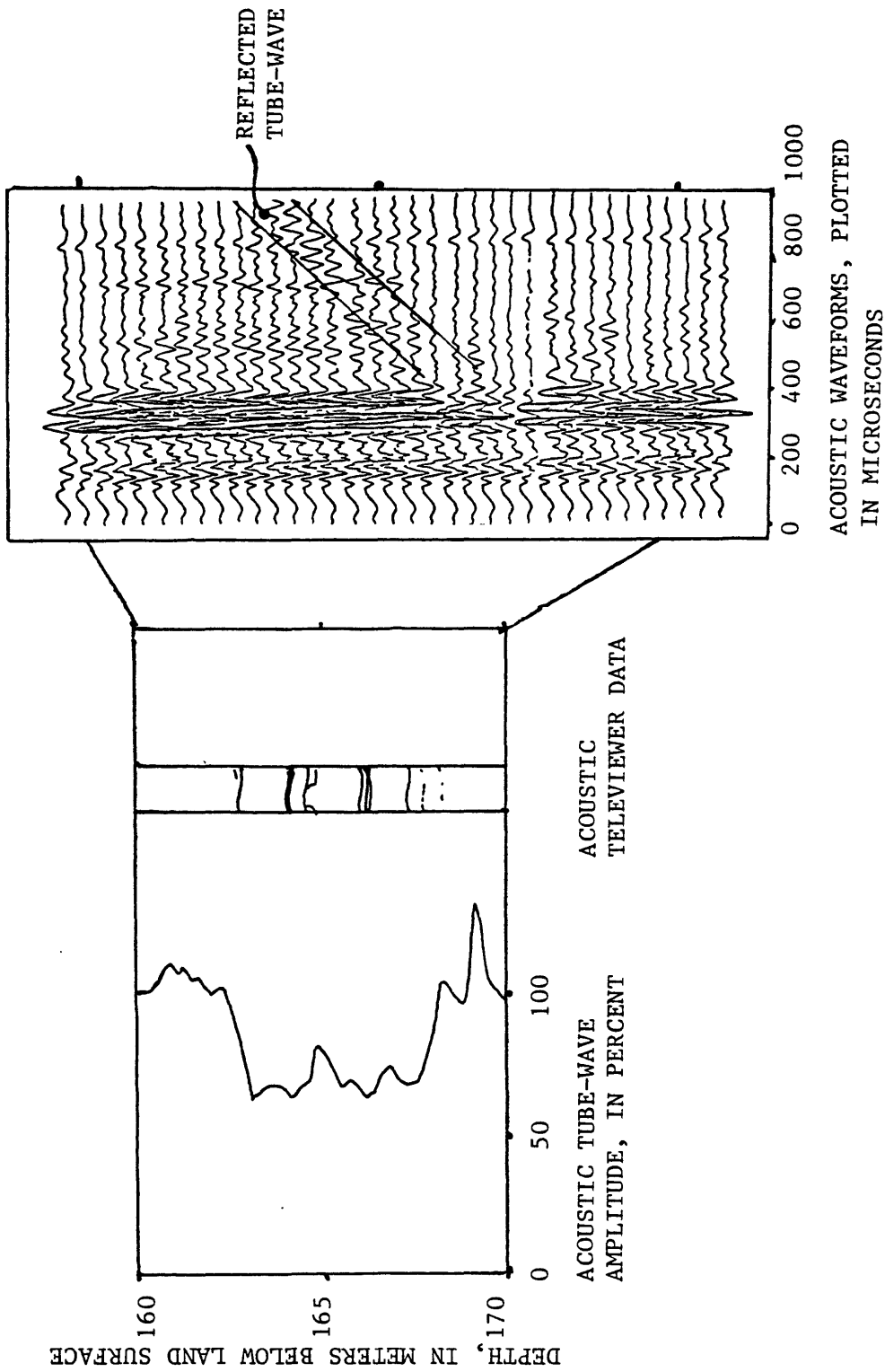
Figure 17.--Acoustic full-waveform data compared to tube-wave amplitude and televiewer logs for isolated fracture set in borehole WRA1; data obtained with 5-kHz sparker source, showing reflected tube-wave above fracture zone.

All tests of the heat-pulse flowmeter with packer system were made in borehole WN1 while waiting for boreholes URL13 and WRA1 to become available. These tests were made in an interval of borehole WN1 where natural downward flow was known to be occurring (Davison and others, 1982). Initial tests with the packer left uninflated produced a heat-pulse travel time of approximately 50 s downward. This represents the time for the heat pulse to convect from the source grid downhole approximately 2 cm to a thermistor (Hess, 1982). Previous experience indicates that travel times approaching 60 s represent the lower limit of flow resolution for this instrument. Measurements in the same position with packer inflated gave heat-pulse travel times of 12 s downward, indicating a significant increase in flow sensitivity. Even with the relatively small annulus between the flowmeter and the borehole wall, this decrease in travel time represents a major improvement in flow resolution. However, repeat measurements indicated that the packer did not remain inflated for more than a few seconds. Further testing of the small-diameter packer system was discontinued. Additional testing of the system with an improved valve design was expected to be completed during 1987.

A few heat-pulse flowmeter measurements without the packer system were made in borehole WRA1, where some natural flow appeared to be occurring. The measurements produced heat-pulse travel times in the range of 50 to 70 s downflow. The flow appeared to enter the borehole at depths less than 80 m, and continued down to the fracture zone ranging in depth from 700 to 750 m. The poor resolution provided by the flowmeter without packer at these low flow rates required extensive periods for stabilization between measurements, so that time constraints kept flowmeter measurements to a very limited set.

SUMMARY

Geophysical well logs were obtained in two deep, fully cored boreholes located on the Canadian shield in southeastern Manitoba in order to investigate measurement techniques and data processing methods for the characterization of potential nuclear waste repositories. One borehole, WRA1, contained multiple zones of fracture permeability: it was used as a case study for the acoustic waveform log interpretation of fracture permeability. Neutron, acoustic transit-time, and single-point resistance logs were the most useful among the conventional geophysical logs for the identification of fractures and alteration adjacent to fractures. The acoustic data were processed by calculating the tube-wave amplitude, and relating local decreases in amplitude to the equivalent single-fracture aperature of an infinite plane fracture. The detailed distribution of equivalent single-fracture permeability in borehole WRA1 was then averaged into the total effective hydraulic transmissivity of 15-m intervals. This interval was selected as representative of intervals likely to be used to conduct future packer isolation and injection tests and to confirm the permeability estimates given in this report. However, the cubic law for hydraulic flow in fractures is used to show how transmissivity values or equivalent single-fracture apertures could be calculated for comparison with packer tests, run using arbitrary isolation intervals.

A second borehole, URL13, penetrated many hundreds of meters of unfractured rocks, providing a useful test of geophysical logs in the detection and characterization of minor changes in lithology and sealed fractures that might be useful in identifying geologic horizons suitable for the development of a radioactive-waste repository. The geophysical logs in borehole URL13 confirmed the homogenous, fracture-free character of many zones within that borehole. However, a significant anomaly in the neutron and acoustic-waveform logs at a depth of about 914 m in borehole URL appeared to indicate a local zone of substantial fracture permeability not indicated by either the other geophysical logs or the core description. Inspection of the acoustic waveform logs indicates that fracture permeability is not likely in this zone even though significant acoustic tube-wave amplitude attenuation occurs. The large anomaly on the neutron is explained otherwise by the observation of a thin mafic dike intersecting the core at approximately 914 m deep in borehole URL13. The anomalous nature of the acoustic log at this depth is the object of intensive on-going including repeat acoustic-waveform logging, televiewer logging, and additional core inspection.

REFERENCES

Aguilera, Roberto, 1979, Naturally fractured reservoirs: Tulsa, Okla.,
    Petroleum Publishing, 703 p.

Anderson, R.N., and O'Malley, H., 1985, Frequency response and attenuation
    changes across highly altered fracture zones crosscutting a fast
    formation: Society of Professional Well Log Analysts Annual Logging
    Symposium, 26th, Dallas, Tex., 1985, Transactions, p. LLL1-12.

Cheng, C.H., and Toksoz, M.N., 1981, Elastic wave propagation in a fluid
    filled borehole and synethetic seismograms: Geophysics, v. 46, no. 7,
    p. 1046-1053.

Davison, C.C., Keys, W.S., and Paillet, F.L., 1982, Use of borehole
    geophysical log and hydrologic tests to characterize crystalline rock for
    nuclear waste storage, Whiteshell Nuclear Research Establishment, Manitoba,
    and Chalk River Nuclear Laboratory, Ontario, Canada: U.S. Department of
    Energy, issued by the U.S. Department of Commerce, National Technical
    Information Service, rept. ONWI-418, 103 p.

Gough, D.I., and Bell, J.S., 1981, Stress orientation from oil-well fractures
    in Alberta and Texas: Canadian Geotechnical Journal, v. 18, no. 6,
    p. 638-645.

Hearst, J.R., and Nelson, P.H., 1985, Well logging for physical properties:
    McGraw-Hill, New York, 571 p.

Hess, A.E., 1982, A heat-pulse flowmeter for measuring low velocities in
    boreholes: U.S. Geological Survey Open-File Report 82-699, 39 p.

-----1986, Identifying hydraulically conductive fractures with a slow-
    velocity heat-pulse flowmeter: Canadian Geotechnical Journal, v. 23,
    no. 1, p. 69-78.

Hillary, E.M., and Hayles, J.G., 1985, Correlation of lithology and fracture
    zones with geophysical borehole logs in plutonic rocks: Atomic Energy
    of Canada Limited Technical Record TR-343, 59 p.

Keys, W.S., 1979, Borehole geophysics in igneous and metamorphic rocks:
    Society of Professional Well Log Analyst Annual Logging Symposium, 20th,
    Tulsa, Okla., June, 1979, Proceedings, p. OO1-26.

Keys, W.S., 1984, A synthesis of borehole geophysical data at the Underground
    Research Laboratory, Manitoba, Canada: Department of Energy Report
    BMI/OCRD-15, 43 p.

Keys, W.S., and MacCary, L.M., 1971, Applications of borehole geophysics to
    groundwater investigations: U.S. Geological Survey Techniques of Water
    Resources Investigations, Bk. 2, Chap. E1, 126 p.

Kierstein, R.A., 1983, True location and orientation of fractures logged with the acoustic televiewer: U.S. Geological Survey Water Resources Investigations Report 83-4275, 71 p.

Lau, J.S.O., 1983, The determination of true orientations of fractures in rock cores: Canadian Geotechnical Journal, v. 20, no. 3, p. 221-227.

Mathieu, Frederic, 1984, Application of full waveform logging data to the estimation of reservoir permeability: Masters Thesis, Department of Earth and Planetary Sciences, Cambridge, Mass., Massachusetts Institute of Technology, 69 p.

Mathieu, Frederic, and Toksoz, M.N., 1984, Application of full waveform acoustic logging data to the estimation of reservoir permeability: Society of Exploration Geophysicists, 54th International Meeting, Atlanta, Georgia, December, 1984, Proceedings, p. 9-12.

Nelson, P.H., Magnusson, K.A., and Rachiele, R., 1983, Applications of borehole geophysics at an experimental waste storage site: Geophysical Prospecting, v. 30, no. 4, p. 910.

Paillet, F.L., 1980, Acoustic propagation in the vicinity of fractures which intersect a fluid-filled borehole: Society of Professional Well Log Analysts Annual Logging Symposium, 21st, Lafayette, La., 1980, Transactions, p. DD1-33.

-----1983, Acoustic characterization of fracture permeability at Chalk River, Ontario: Canadian Geotechnical Journal, v. 20, no. 3, p. 468-476.

-----1984, Field tests of an acoustic sparker source for waveform logging: Society of Professional Well Log Analysts Annual Logging Symposium, 25th, New Orleans, La., 1984, Transactions, p. GG1-22.

-----1985a, Problems in fractured-reservoir evaluation and possible routes to their solution: Log Analyst, v. 26, no. 6, p. 26-41.

-----1985b, Geophysical well log data for study of water flow in fractures in bedrock near Mirror Lake, New Hampshire: U.S. Geological Survey Open-File Report 85-340, 27 p.

Paillet, F.L., and Hess, A.E., 1987, Geophysical well log analysis of fractured granitic rocks at Atikokan, Ontario, Canada: U.S. Geological Survey Water Resources Investigations Report 87-4154, 36 p.

Paillet, F.L., Cheng, C.H., Hess, A.E., and Hardin, E.L., 1986, Comparison of fracture permeability estimates based on tube-wave generation in vertical seismic profiles, acoustic waveform-log attenuation, and pumping-test analysis: National Water Well Association Conference and Exposition, Denver, Colo., 1986, Proceedings, p. 398-416.

Paillet, F.L., and Hess, A.E., 1986, Geophysical well log analysis of
    fractured crystalline rock at East Bull Lake, Ontario, Canada: U.S.
    Geological Survey Open-File Report 86-4052, 37 p.

Paillet, F.L., Hess, A.E., Cheng, C.H., and Hardin, E.L., 1987,
    Characterization of fracture permeability with high-resolution vertical
    flow measurements during borehole pumping: Ground Water, v. 25, no. 1,
    p. 28-40.

Paillet, F.L., and Kim, Kunsoo, 1987, Character and distribution of borehole
    breakouts and their relationship to in situ stresses in deep Columbia
    River basalts: Journal of Geophysical Research, v. 92, no. B7,

Paillet, F.L., Keys, W.S., and Hess, A.E., 1985, Effects of lithology on
    acoustic televiewer log quality and fracture interpretation: Society
    of Professional Well Log Analysts Annual Logging Symposium, 26th,
    Dallas, Tex., 1985, Transactions, p. JJJ1-31.

Paillet, F.L., and White, J.E., 1982, Acoustic normal modes of propagation
    in the borehole and their relationship to rock properties: Geophysics,
    v. 47, no. 8, p. 1215-1228.

Rosenbaum, J.H., 1974, Synthetic microseismograms - logging in porous
    formations: Geophysics, v. 39, no. 1, p. 14-32.

Snow, D.T., 1965, A parallel plate model of fractured permeable media:
    Ph.D. Thesis, University of California, Berkeley, 81 p.

Witherspoon, P.A., Tsang, Y.W., Long, J.C.S., and Jahandar, Norrishad, 1981,
    New approaches to problems of fluid flow in fractured rock masses:
    Symposium on Rock Mechanics, 22d, Cambridge, Mass., 1981, Proceedings,
    p. 3-22.

Zemanek, Joseph, Caldwell, R.L., Glenn, E.E., Halcomb, S.V., Norton, L.J.,
    and Strauss, A.J.D., 1969, The borehole televiewer--a new logging
    concept for fracture location and other types of borehole inspection:
    Journal of Petroleum Technology, v. 21, no. 6, p. 762-774.

Zoback, M.D., Moos, D., Mastin, L., and Anderson, R.N., 1985, Well bore
    breakouts and in situ stress: Journal of Geophysical Research, v. 90,
    no. B12, p. 5523-5530.